Public

Report

Document ID	Version	Status	Reg no	Page
1404369	2.0	Approved		1 (59)
Author: Jan Hernelind/5T Engineering AB			Date: 2014-03-07	
Reviewed by			Reviewed date	
Approved by: Jan Sarnet			Approved date: 2014-03-14	

Modelling of a canister with broken insert subjected to earthquake induced shear and subsequent glacial load

Overview

This report is one in a series of reports that together address the response of the buffer and the canister in a KBS-3 repository to shear movements in fractures intersecting deposition holes. The purpose with this study is to investigate the effect on the copper shell and especially if the copper shell will withstand the extremely pessimistic assumptions made for these analyses.

Rock shear movements to analyse are given as design requirements derived from previous safety assessments. Mechanical properties of the buffer are determined in laboratory tests that are interpreted into a buffer material model with parameter values for the calculations. Mechanical data for the canister insert and copper shell are obtained from laboratory tests yielding canister material models.

In this study the effect on the copper shell is analyzed when the rock shearing has caused a complete failure of the insert including the steel channel tubes. The analysis is simplified by assuming that the insert initially has a crack going through the insert and the channel tubes. The rock shear deformation is then applied followed by a creep analysis.

Abstract

Existing fractures crossing a deposition hole may be activated and sheared by an earthquake. The effect of such a rock shear has been investigated by the finite element code ABAQUS. A three-dimensional element mesh of the buffer and canister has been created for analyzing the rock shearing.

The rock shearing has been assumed to take place perpendicular to the canister at the distance 2/3 from the base of the insert when the insert and channel tubes are assumed to have an entire (insert and channel tubes) crack-through 5^{o} inclined to the normal direction of the centre axis in tension. The shear calculations have been driven to a total shear of 10 cm.

Besides rock shear the model has been used to analyse the effect of increased glaciations pressure of 15 or 45 MPa combined with rock shear when considering creep in the copper shell. The conclusion is that the copper shell will remain as a protection even for these very pessimistic assumptions.

Svensk Kärnbränslehantering AB
Swedish Nuclear Fuel and Waste Management Co
PO Box 925, SE-572 29 Oskarshamn
Visiting address Gröndalsgatan 15
Phone +46-491-76 79 00 Fax +46-491-76 79 30
www.skb.se
556175-2014 Seat Stockholm

Sammanfattning

Befintliga sprickor som skär deponeringshål kan aktiveras och skjuvas genom ett jordskalv. Inverkan av en sådan bergskjuvning har analyserats med finita elementkoden ABAQUS. Ett tredimensionellt elementnät av buffert och kapsel har skapats för analys av bergskjuvningen.

Bergskjuvningen antas ske vinkelrätt mot kapselaxeln med en i insatsen och kanalrören genomgående spricka i 5^{o} vinkel mot kapselaxeln i drag.

Skjuvberäkningarna har genomförts upp till en total skjuvdeformation av 10 cm.

Förutom bergskjuvning har modellen använts för att analysera effekten av en tryckhöjning med 15 och 45 MPa kombinerad med bergskjuvning när hänsyn tas till krypning i kapseln. Slutsatsen är att kopparskalet förblir ett skydd också för dessa mycket pessimistiska antaganden.

Contents

1 Introduction

The canister has to be designed to withstand earthquake induced rock shear of 5 cm and also a glacial load up to 45 MPa. This report describes the effect during loading of the canister from a postulated crack inclined 5 degrees from the normal of the centre axis through the entire insert and channel tubes. One important function of the buffer material in a deposition hole in a repository for spent nuclear fuel disposal is to reduce the damage of rock movements on the canister. The worst case of rock movements is a very fast shear that takes place along a fracture plane and occurs as a result of an earthquake.

The consequences of such rock shear have been investigated earlier, both by laboratory tests (Börgesson et al. 2004), laboratory simulations in the scale 1:10 and finite element modelling (Börgesson et al. 2004) and (Börgesson et al. 1995).

Since it is very probable that the Na-bentonite will be transformed to Ca-bentonite or that Ca-bentonite might be used as buffer, the calculations now are based on material properties of Ca-bentonite instead of Na-bentonite.

This report summarizes the results when the buffer consists of converted Ca-bentonite with density 2,050 kg/m^3.

Both short term response (elastic-plastic material model for copper) and long term response (creep model for copper) has been analyzed.

1.1 Hydrostatic pressure

As stated in the design premises (SKB 2009), the copper corrosion barrier should remain intact after a 5 cm shear movement at a velocity of 1 m/s for buffer material properties of a 2,050 kg/m^3 Ca-bentonite, for all locations and angles of the shearing fracture in the deposition hole, and for temperatures down to 0°C. The insert should maintain its pressure-bearing properties to isostatic loads. The canister shall withstand an isostatic load of 45 MPa, being the sum of maximum swelling pressure and maximum groundwater pressure.
The load is assumed to be applied for a long time which implies that creep of the copper has to be considered.

This report summarizes results for the BWR-canister when the effect of the increased pressure is simulated considering creep in the copper shell.

2 Geometry definitions and meshes

2.1 General

The geometry used in the analysis of the impact of earthquake induced rock shear consists of the insert (made of nodular cast iron), the insert lid (made of steel) and the copper shell surrounded by buffer material (bentonite). The geometry is based on CAD-geometries received from SKB, "Ritningsförteckning för kapselkomponenter" (SKBdoc 1203875) and should therefore correspond to the current design.

Due to symmetry only one half has been modelled. The mesh is then generated by 3-dimensional solid elements, mainly 8-noded hexahedral (most of them using full integration technique) and a few 6-noded wedge.

The model size is defined by about 120,000 elements and 150,000 nodes (total number of variables about 600,000). BWR insert, see Figures 2-1 - 2-2.

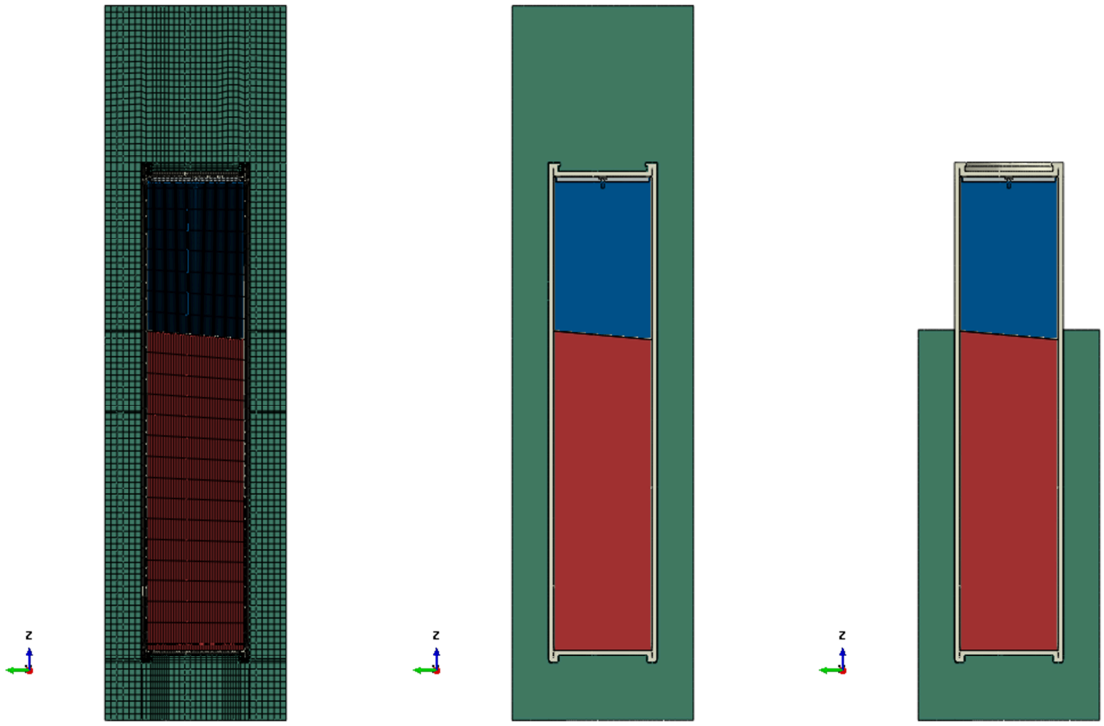

Figure 2-1. *Plot of geometry for rock shear with a crack in the BWR-canister, 85 degrees to axis of canister and 1/3 shearing part removed (right).*

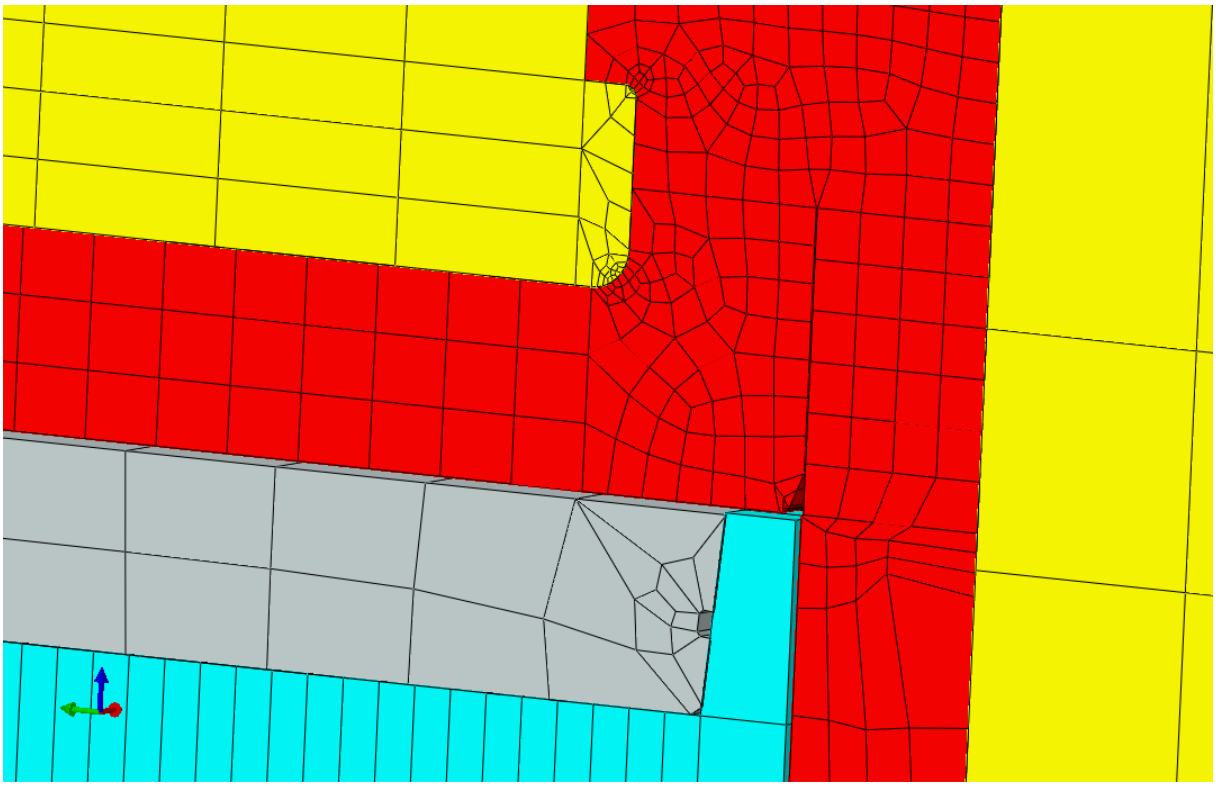

Figure 2-2. *Detail of upper corner showing bentonite (yellow), copper shell (red), insert lid (grey) and insert (cyan).*

2.2 Geometry of parts

2.2.1 Deposition hole

The model of the deposition hole has a diameter of 1.75 m and a length of 6.9 m. The canister is placed about 0.5 m above the bottom and about 1.5 m below the top of the deposition hole. Buffer material (bentonite) surrounds the canister and will fill out the deposition hole. The rock shear is then simulated by prescribing boundary conditions at the buffer envelope.

2.2.2 Insert

The insert is made of nodular cast iron and has been simplified regarding the square tubes which are assumed to be tied to the cast iron insert and thus these contribute as added material to the insert. This simplification will probably overestimate stresses and strains in this region.

The insert (BWR, see Figure 2-4) is modeled as a homogeneous part with 3D solids.

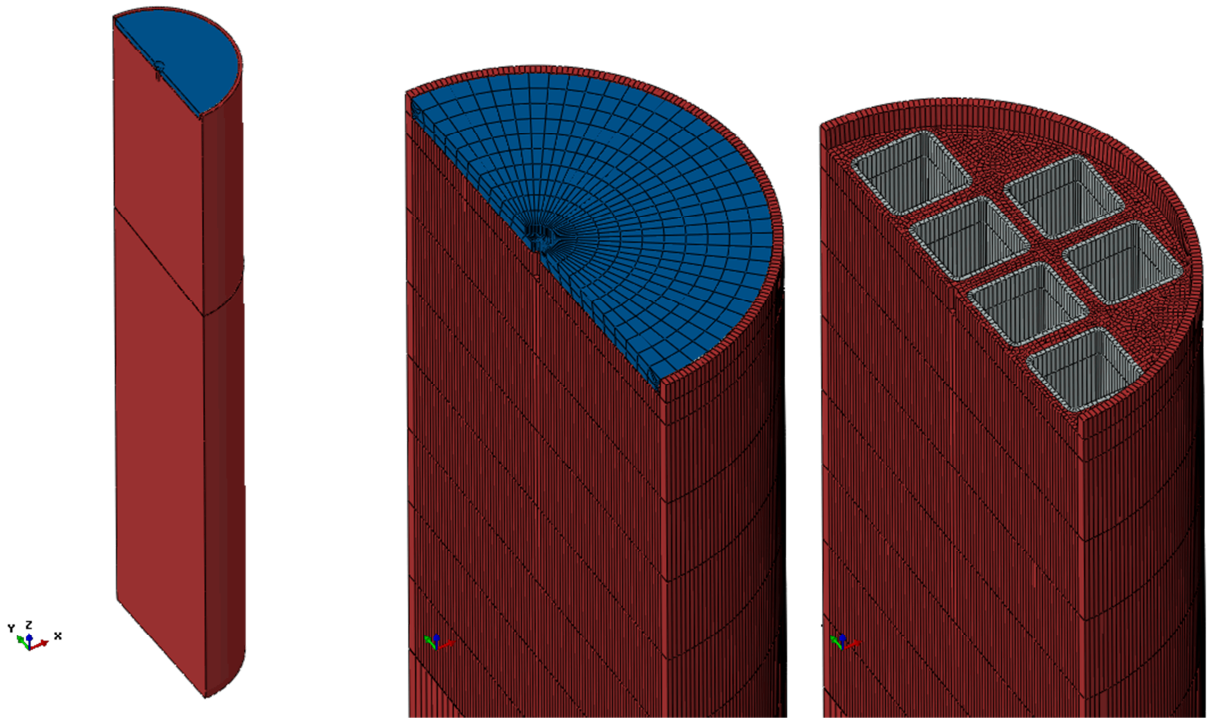

Figure 2-3. *Insert BWR geometry (left), mesh with lid (mid) and without lid (right).*

2.2.3 Steel lid

The insert lid is made of steel and is modelled with 3D solids, see Figure 2-5.

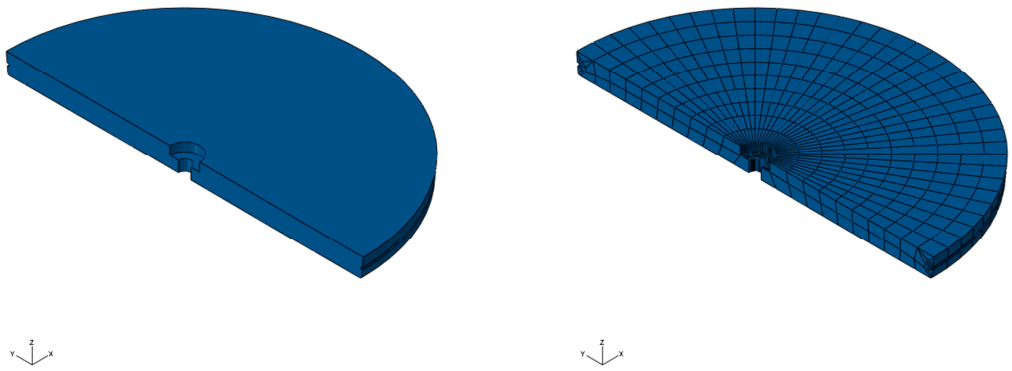

Figure 2-5. *Steel lid geometry (left) and mesh (right).*

2.2.4 Copper shell

The copper shell surrounds the insert and interacts with the buffer and the insert. The canister has been modelled rather accurately in order to catch “hot spots” where large strains are expected, e.g. the fillets at the base and top (the copper lid). The lid is welded to the flange and lid and canister will act as one part, see Figure 2-6.

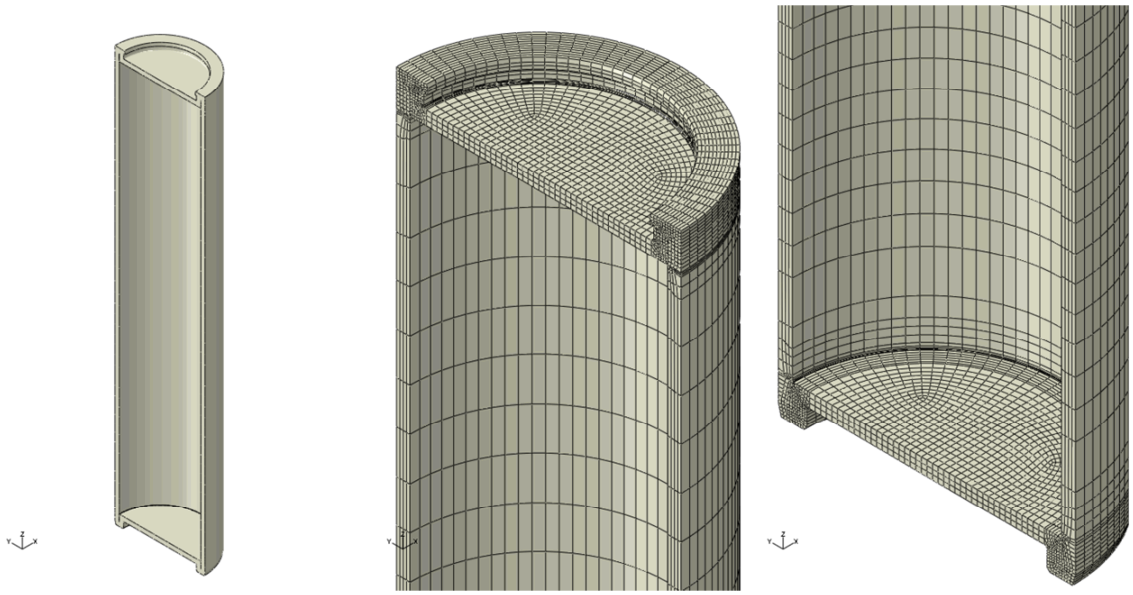

Figure 2-6. *Copper shell geometry (left), mesh top (mid) and mesh base (right).*

3 Material models

The finite element code ABAQUS was used for the calculations. The materials have been modelled as elastic-plastic with stress-strain properties that correspond to each material and the applied shear load induced strain rate, when applicable. The strains obtained from the simulations are below any necking and the material definitions thus cover the range of obtained results.

Note that in ABAQUS values outside the definition range will be constant with the last value defined.

3.1 Nodular cast iron (used for the BWR-insert)

The material model for the insert is based on a von Mises' material model with elastic behaviour defined by Young's modulus and the Poisson's ratio and the plastic behaviour defined through yield surface (true stress) versus plastic strain (defined as logarithmic strain), see Table 3-1 and Figure 3-1 (SKBdoc 1201865).

Data is available up to 15% plastic equivalent strain which covers the range of obtained results for the performed analyses.

The experiments were performed at 0°C.

Table 3-1. Stress-strain definition for BWR-insert.

Plastic Strain (%)	Stress (MPa)			
	Strain rate=0/s	Strain rate=2×10^{-4}/s	Strain rate=0.5/s	Strain rate factor at strain rate=0.5/s
0	293	293	348	1.19
1	324	324	367	1.13
2	349	349	385	1.10
3	370	370	406	1.10
4	389	389	423	1.09
5	404	404	438	1.09
6	418	418	451	1.08
7	428	428	464	1.08
8	438	438	474	1.08
9	447	447	483	1.08
10	456	456	490	1.07
11	465	465	498	1.07
12	472	472	504	1.07
13	478	478	510	1.07
14	484	484	516	1.07
15	488	488	520	1.07

The strain rate dependency is defined by assuming that the yield surface is proportional to the strain rate factor (at the strain rate 0.5/s the factor 1.08 has been chosen and at strain rate 0/s the factor is 1.0).The instantaneous strain rate factor is then linearly interpolated between 1 and 1.08 using the instantaneous strain rate.

Furthermore, Young's modulus E = 166 GPa and Poisson's ratio ν = 0.32 (Raiko et al. 2010).

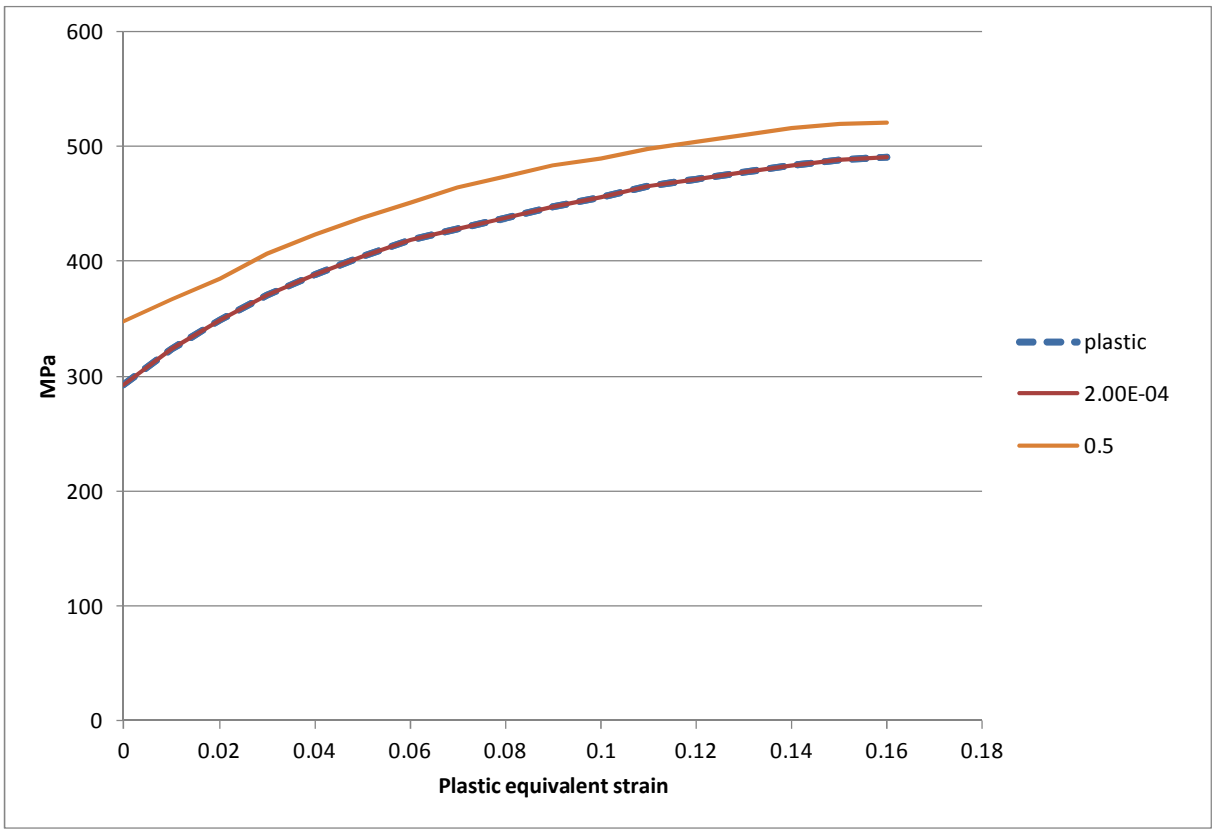

Figure 3-1 *Insert yield surface (nodular cast iron), true stress, [MPa] versus logarithmic plastic equivalent strain for different plastic strain rates. Note that the base (plastic) is defined to coincide with strain rate=2×10^{-4} /s.*

3.2 Steel (used for the channel tubes in the insert)

The material model for the channel tubes in the insert is based on a von Mises' material model with elastic behaviour defined by Young's modulus and the Poisson's ratio. The plastic behaviour is defined through yield surface (true stress) versus plastic strain (using logarithmic strain).

The steel cassette tubes are manufactured by steel S355J2H, for example Domex 355 MC B. SKB has earlier supplied test data for the yield point of their material, however no stress-strain data to be used in a plastic analysis. The stress-strain curve for Domex 355 MC B (SSABDirekt 2008) can be scaled using the yield stress and tensile ultimate strength measured by SKB, *Re* = 412 MPa and *Rm* = 511 MPa. With this procedure a simplified stress-strain curve is obtained and described by Table 3-2 and Figure 3-2.

Table 3-2. Stress-strain definition for channel tubes used in the insert.

Strain (%)	Stress (MPa)	Log Strain (%)	True Stress (MPa)	Plastic equivalent strain (%)
0	0	0	0	0
0.196	412	0.196	412	0
15	509	14.3	587	14.0
20	511	18.5	613	18.2

Furthermore, Young's modulus E = 210 GPa and Poisson's ratio ν = 0.33 according to Raiko et al. table 4-3 (2010).

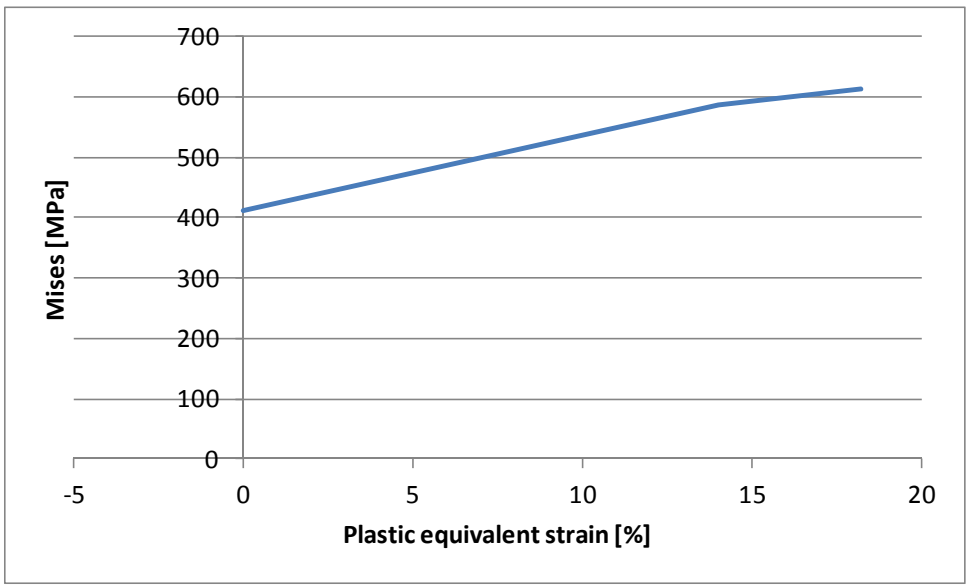

Figure 3-2. *Channel tube yield surface, true stress [MPa], as a function of the logarithmic plastic equivalent strain.*

The data with lowest value from the experiment has been chosen for the yield surface. However, the plasticity definition for the steel channel tubes has very minor influence on the overall results. Furthermore the obtained results from the performed analyses are within the range for available material data.

3.3 Steel (used for the insert lid)

The material model for the insert lid is based on a von Mises' material model with elastic behaviour defined by Young's modulus and the Poisson's ratio. The plastic behaviour is defined through yield surface (true stress) versus plastic strain (calculated as logarithmic strain).

Manufacturing drawings for the lid specify steel S355J2G3. Strain versus stress for steel Domex 355 MC B with Re = 389 MPa and Rm = 484 MPa can be found from (SSABDirekt 2008). According to (SKBdoc 1201865) the material S355 with nominal thickness 40-63 mm has Re = 335 MPa and Rm = 470-630 MPa. Scaling stress-strain curves for Domex 355 by the minimum values given in (SS-EN 10025 del 2, 2004) implies the following simplified material definition (engineering data) shown in Table 3-3 and Figure 3-3.

Table 3-3. Stress-strain definition for the steel lid.

Strain (%)	Stress (MPa)	Log Strain (%)	True Stress (MPa)	Plastic equivalent strain (%)
0	0	0	0	0
0.1595	335	0.1593	335	0
15	470	13.98	540	13.7
20	470	18.2	564	17.9

Furthermore, Young's modulus E = 210 GPa and Poisson's ratio ν = 0.3 according to Raiko et al. Table 4-3 (2010).

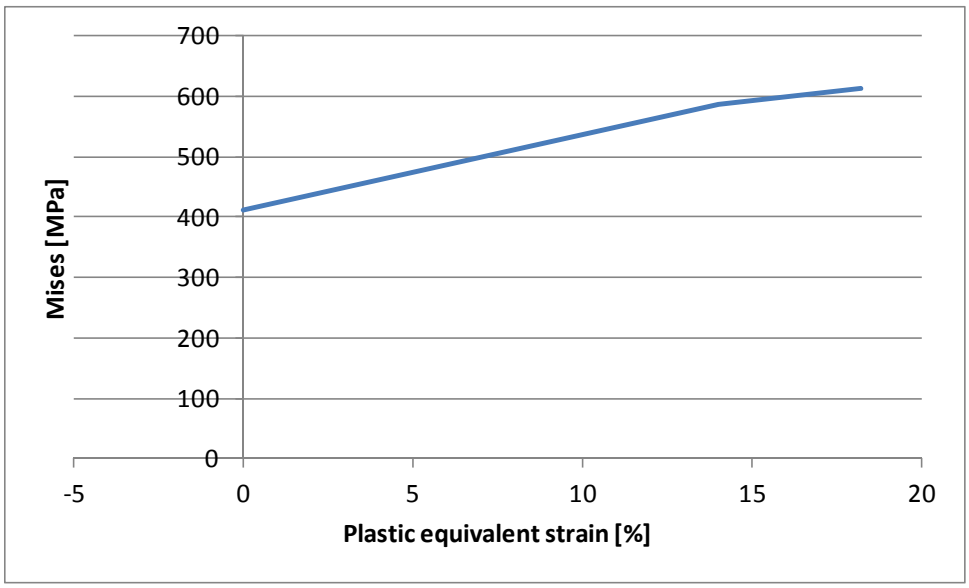

Figure 3-3. *Insert lid yield surface, true stress [MPa], as a function of the logarithmic plastic equivalent strain.*

The data with lowest value from the experiments (SS-EN 10025 del 2, 2004) has been chosen for the yield surface. However, the plasticity definition for the insert lid has very minor influence on the overall results. Furthermore, the obtained results are within the range of available material data.

3.4 Bentonite model (used for the buffer)

The bentonite is modelled based on recent experiments, see (Börgesson et al. 2010) and adapted to the actual density of the bentonite. The bentonite buffer is modelled using only total stresses that do not include the pore water pressure, the reason being the very fast compression and shear.

The most important properties of the bentonite for the rock shear are the stiffness and the shear strength. These properties vary with bentonite type, density and rate of strain. Ca-bentonite has higher shear strength than Na-bentonite and the shear strength increases with increasing density and strain rate. Since it cannot be excluded that the Na-bentonite MX-80 will be ion-exchanged to Ca-bentonite the properties of Ca-bentonite is used in the modelling. The acceptable density at saturation of the buffer material is 1,950 kg/m^3 – 2,050 kg/m^3 which is covered by the models below.
The material model is in ABAQUS expressed with the von Mises' stress σ_j that describes the "shear stress" in three dimensions according to Equation 3-1.

$$\sigma_j=(((\sigma_1-\sigma_3)^2+(\sigma_1-\sigma_2)^2+(\sigma_2-\sigma_3)^2)/2)^{1/2} \quad (3\text{-}1)$$

where

σ_1, σ_2 and σ_3 are the principal stress components.

The material model defines the relation between the stress and the strain and is partitioned in elastic and plastic parts. For details regarding definition of the shear strength and the influence of density, pressure and rate of shear see (Börgesson et al. 1995) and (Börgesson et al. 2004).

Rate dependent elastic-plastic stress-strain relation
The elastic-plastic stress strain relations used for the three different densities are derived according to the description above in an identical way as the relations used in all previous calculations.

The bentonite is modelled as linear elastic combined with the von Mises' plastic hardening - Table 3-4 shows the elastic constants. The plastic hardening curve is made a function of the strain rate of the material. The reason for the latter relation is that the shear strength of bentonite is rather sensitive to the strain rate. It increases with about 10% for every 10 times increase in strain rate. Since the rock shear at an earthquake is very fast (1 m/s) the influence is strong and the resulting shear strength will be different at different parts of the buffer. Figure 3-4 shows the material model. The stress-strain relation is plotted at different strain rates.

Table 3-4. Elastic material data for the bentonite buffer Na converted to Ca.

Density (kg/m^3)/Swelling pressure (MPa)	Elastic part	
	E (MPa)	ν
1950/5.3	243	0.49
2000/8	307	0.49
2050/12.3	462	0.49

The experiments (Börgesson et al. 2010) show that also Young's modulus (E) is dependent on strain rate but in the calculations this has been neglected and a representative stiffness has been chosen (sensitivity analyses did show minor changes of the results when varying Young's modulus between maximum and minimum values achieved from the experiments).

From the performed analyses it is obvious that the bentonite gets plastic strains outside the defined range for material data. However, other studies (SKBDoc 1407337) show that this does not affect the results significantly.

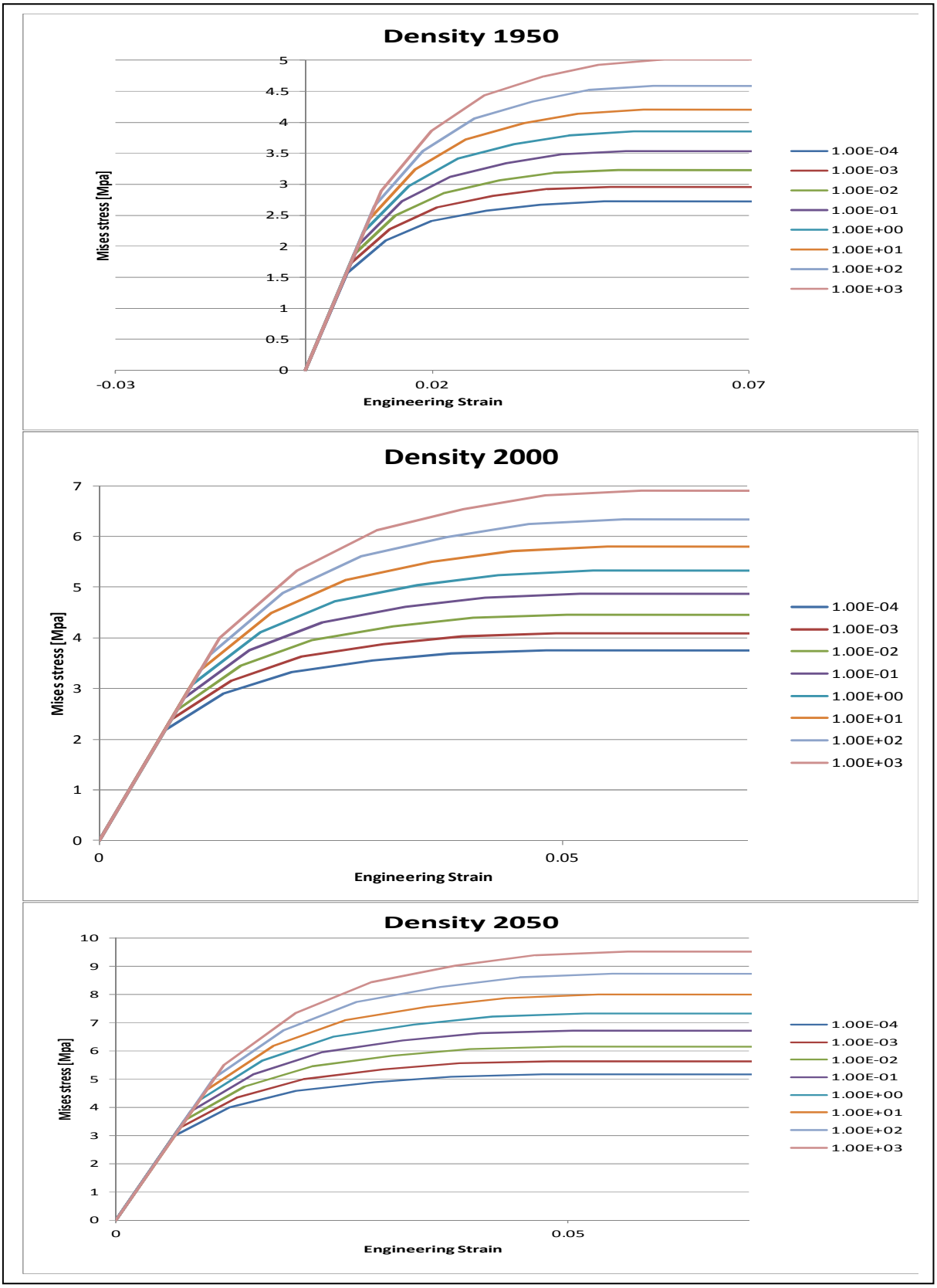

Figure 3-4. *Plot of material definition for the bentonite buffer for different densities (kg/m^3) and strain rates (/s). Mises stress [MPa] versus engineering strain.*

3.5 Copper model

3.5.1 Kimab material

The material model used for copper for most of the global analyses is described below.
The stress-strain properties of the copper in the copper shell were investigated by the Corrosion and metals research institute Swerea Kimab and the results were then represented by a creep material model developed by Rolf Sandström, see (Sandström and Andersson 2008), (Jin and Sandström 2008) and (Sandström et al. 2009).

The material model for the short duration rock shear analysis, used for all analyses in this study and also in previous studies for short duration rock shear analyses (Hernelind 2010) and (SKBdoc 1339902), is based on a simplified elastic-plastic material model, see Table 3-5, using data from the creep model assuming a strain rate of 5×10^{-3}/s which is considered as conservative.

The flow curve data has been calculated from (Sandström et al. 2009) wherein eq.(17) has been used together with the parameter values defined in the corresponding Table 4-2, (Sandström et al. 2009) as well as $m = 3.06$, $\alpha = 0.19$, $\omega = 14.66$.

The copper model data is shown in Figure 3-5. Data is available up to 50% and covers the range of obtained results.

Table 3-5. Elastic-plastic material data for the copper at strain rate 5×10^{-3}/s.

Elastic part		Plastic part: von Mises stress σ_j (MPa) at the following plastic strains (ε_p)					
E (MPa)	ν	0	0.10	0.20	0.30	0.40	0.50
$1.2\cdot10^5$	0.308	72	178	235	269	288	300

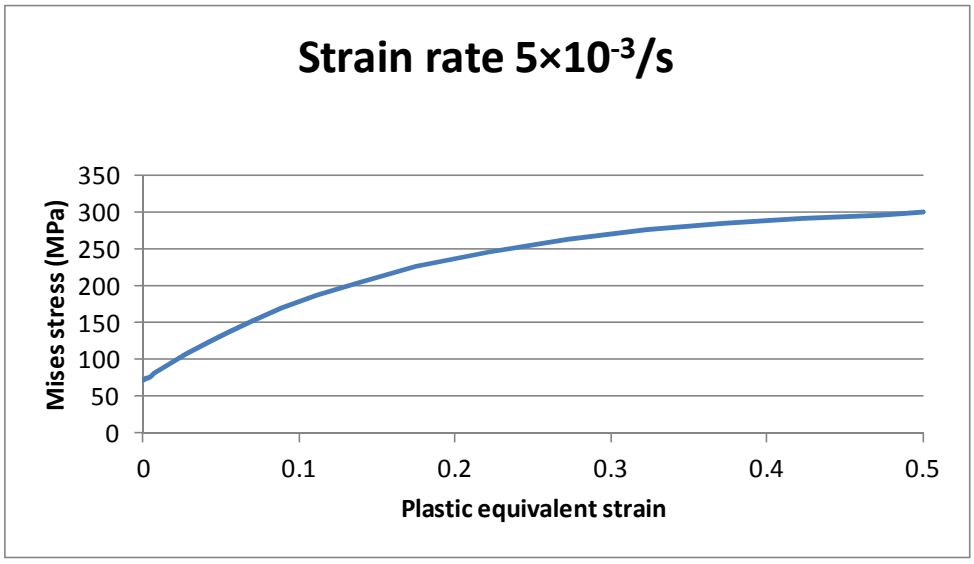

Figure 3-5. *Copper shell yield surface, true stress, [MPa] as a function of the logarithmic plastic equivalent strain.*

Also long term duration has been simulated using the creep model implemented in ABAQUS as a user supplied subroutine (CREEP) which is essentially based on eqn 10-1 in (Andersson-Östling and Sandström 2009).

4 Contact definitions

All the boundaries of the buffer, the copper shell, the insert and the insert lid interact through contact surfaces allowing finite sliding. All contact surfaces have friction at sliding with no cohesion and the friction coefficient 0.1, i.e. the friction angle and cohesion are:

$\phi = 5.7^{\circ}$

c=0 kPa

Since the actual value for the coefficient of friction is uncertain for the insert fracture, a sensitivity analysis has been performed by also using the values 0.0 and 0.2.

The contact is released when the contact pressure is lost.

A few contact pairs are tied together (tied means that the surfaces are constrained together and will not allow for opening/closing or sliding) in order to improve the numerical convergence rate. This applies at the contact pairs between the insert and insert lid and also at the base of insert and copper shell bottom.

The interaction between the buffer and the rock (not modelled) is assumed to be tied through prescribed boundary conditions and will not allow for opening/closing or sliding.

5 Initial conditions

Initial conditions are defined as:

- Temperature for all nodes in the model as 300 K (only used for the creep analysis and is used by the user defined creep material). The temperature is assumed not to change during the analysis.

- Total pressure for the buffer (17.3 MPa) based on the swelling pressure (12.3 MPa for bentonite with density 2,050 kg/m^3) plus 500 meter water pressure (5 MPa) when using elastic-plastic material model without pore pressure. Since the canister deforms when the initial stresses are applied, the calculated magnitude of the swelling pressure will decrease. For that reason the initial condition for pressure is given as 40.2 MPa based on the obtained pressure (about 17.3 MPa) after equilibrium iterations. At the start of rock shearing simulation the pressure on the outer surface of the copper shell thus is about 17.3 MPa. Another observation is that the calculated swelling pressure will vary both in the axial and radial direction which means that it's not possible to have the correct swelling pressure without using elements with pore pressure as a degree of freedom (ABAQUS have those elements but the material model is tuned to total stresses and not effective stresses).

- Internal solution dependent variables (SVAR) have been initialized to zero when using the user defined creep material.

6 Boundary conditions

Symmetry conditions have been specified for the symmetry plane (displacements in the normal direction to the symmetry plane prescribed to zero), see Fig 6-1. Furthermore, when the effect of long term creep with additional hydrostatic pressure load is analyzed, the rigid body motion has been constrained by prescribing the displacements to zero at the axis of symmetry at one point in the axial direction and at two points in the horizontal direction, see Figure 6-2. The strategy for this case is explained later.

The surrounding rock has been simulated by prescribing the corresponding displacements at the outer surface of the buffer and depends also on type of simulation.

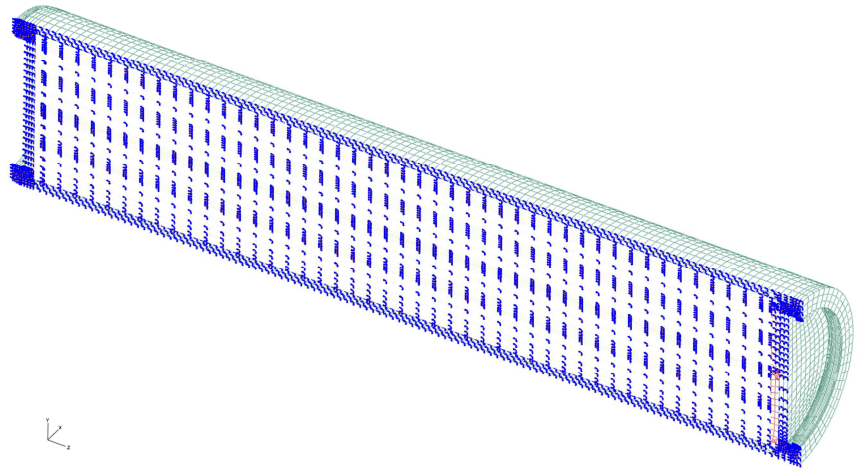

Figure 6-1. *Prescribed symmetry conditions.*

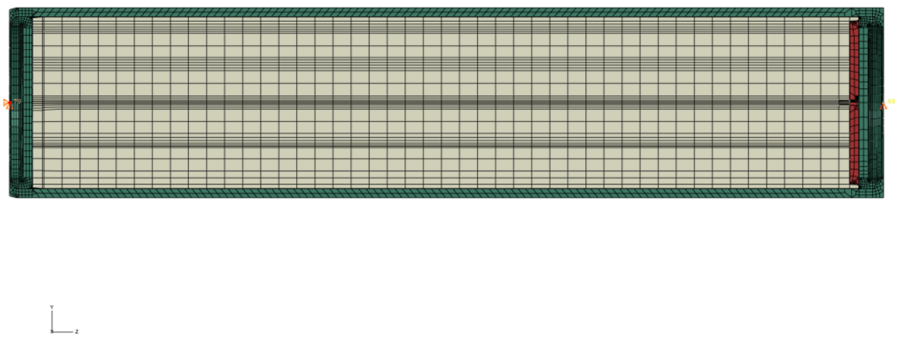

Figure 6-2. *Boundary conditions (red dots) to avoid the rigid body motion, when the buffer is not modelled at all.*

7 Calculations

7.1 Rock shear calculation cases

In the analyses the buffer is based on Na-bentonite converted to Ca-bentonite with density 2,050 kg/m^3.

One case of rock shear directions has been analyzed – the direction has been chosen based on the results from previous analysis:

- **rock shear perpendicular to the axis of the canister** at 2/3 of the height from the base (model7_normal_third_2050ca3 and model7_normal_third_highfriction_2050ca3)

The long term scenario with 15 or 45 MPa hydrostatic pressure (these loads have been applied directly to the outer surface of the copper shell) has also been analyzed where creep effects are included for the copper shell (model7_normal_third_creep1_2050ca3 followed by model7_normal_third_creep1_2050ca3_r1) when the buffer is removed and replaced by the reaction forces corresponding to equilibrium when removing the buffer.

Also another approach has been used where the buffer is active during the long term scenario – 15 MPa is applied to the outer surface of the copper shell also for this case. (model7_normal_third_creep1_relax_2050ca3 for 5 cm rock shear and model7_normal_third_creep_relax_2050ca3 for 10 cm rock shear).

When 45 MPa is applied to the outer surface of the copper shell model7_normal_third_creep1_45_relax_2050ca3 for 5 cm rock shear and model7_normal_third_creep45_relax_2050ca3 for 10 cm rock shear are used.

7.1.1 Analysis approach

The numerical calculations are performed using the FE-code ABAQUS (ABAQUS 2008) version 6.10 assuming non-linear geometry and material definitions. This means that all non-linearities defined by the input will be considered such as large displacements, large deformations, non-linear interactions (contact) and non-linear materials.

All non-linear contributions will be used when forming the equations to be solved for each equilibrium iteration.

Short term analysis is based on static response and the results will not depend on the time used for the simulation except if rate-dependent material data is used.

Long term analysis is based on static response and the results will depend on the time used for the simulation.

The code will choose suitable time-increments for the loading based on (in most cases) default convergence tolerances.

The long term analysis (100,000 years) is performed with the applied hydrostatic pressure.

7.2 Short term analyses

The short term analyses (few seconds) consist of three steps where the shearing is prescribed by boundary conditions. In the first step, initial stresses are applied to achieve a pressure onto the copper shell corresponding to the swelling pressure (12.3 MPa for bentonite with density 2,050 kg/m^3) plus 5 MPa hydrostatic pressure (the deposition is made about 500 meters below the surface). In the second step, 5 cm is used for the shearing magnitude followed by further 5 cm shearing magnitude in the third step.

The results for BWR are shown in Appendix 1-2 for density 2,050 kg/m^3.

7.3 Long term analyses with creep in copper included

The long term analyses (100,000 years) are performed by using the full symmetric model.

The results for the long term analyses are shown in Appendix 3 (model7_normal_third_creep_2050ca3).

Two different approaches have been used:

1 – an earthquake induced rock shearing has been applied (5 cm respectively 10 cm) followed by a restart where the bentonite is removed and instead the corresponding forces has been applied to the surface of the copper shell. In the next step the hydrostatic pressure (15 MPa) has been applied onto the surface of the copper shell for a short period of time (1000 s) followed by a relaxation analysis for 100,000 years. These analyses were not possible to complete due to rapidly increasing creep strains in the copper shell – most probably is the absent of a stabilizing buffer the reason for convergent difficulties. However, it is still interesting to compare with the second approach below since this approach has a more accurate definition of the applied loads.

2 – an earthquake induced rock shearing has been applied (5cm respectively 10 cm). In the next step the hydrostatic pressure (15 or 45 MPa) has been applied onto the surface of the copper shell for a short period of time without removing the buffer material (this is considered to be a more realistic approach). The final step is a relaxation analysis for 100,000 years which did complete without any major difficulties.

The creep material model requires extremely small time increments if the model contains singularities. The analysis will run much faster if instead a plasticity model is used in these regions, see Figure 7-1.

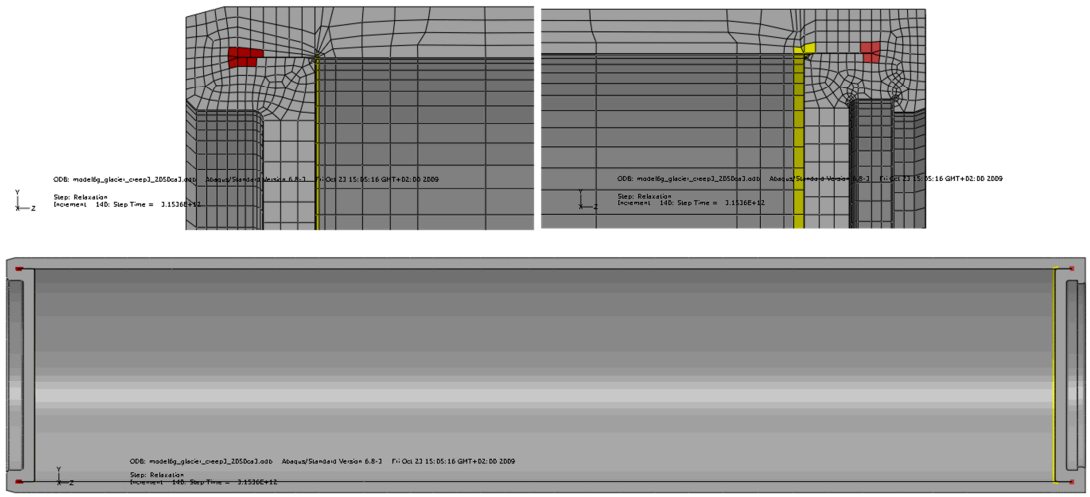

Figure 7-1*. Material definition regions for the copper shell. Red and yellow regions using plasticity, otherwise the creep model is used.*

8 Results

For each analysis a large amount of results are available and to have an indication only a few values are reported.

8.1 Results for rock shearing (BWR)

For the short term rock shear analyses the peak values for Mises' stress and plastic strain (PEEQ) are summarized in Tables 8-1 to 8-5 and the long term response is summarized in Tables 8-8 to 8-11.

Nodular cast iron insert

The highest value for PEEQ in the cast iron insert, 2.2%, and in the steel channels, 3.2%, occurs when the high coefficient of friction is used and the rock shearing magnitude is 10 cm. When the creep material model is used for the copper shell the highest value for PEEQ in the cast iron insert is 6% with rock shearing magnitude of 10 cm and if the buffer is removed the highest value of PEEQ is 5% already after 36 days (where the analysis stops due to convergence difficulties).

For the cast iron insert the failure criteria is based on J-integral but the critical region for initial cracks are chosen based on stress level (maximum axial tension stress, S33) and thus Table 8-1 also contains the corresponding global stresses. As can be seen the highest value is 278 MPa (high friction) and 318 MPa if the creep material model is used for the copper shell. However, since the insert is assumed to be initially broken the obtained stress level is low.

Copper shell

The peak values for plastic strain occur at a few "hot spots" and therefore the results for the copper shell are reported for nine regions (in the cylindrical part, in areas containing the welds (top and bottom), in areas containing geometric discontinuity (top and bottom), the fillet regions (top and bottom) and finally the remaining regions (top and bottom), see Figure 8-1. The summary of results is listed in Tables 8-2 to 8-5 for the short term rock shear analyses and in Tables 8-8 to 8-11 for the long term analyses.

For the short term analyses the highest value for PEEQ in the copper shell is 17% at 5 cm rock shearing magnitude when high friction is used for the fracture surface and 19.3% at 10 cm rock shearing magnitude when low friction is used for the fracture surface. However, the largest values are at the welds and at regions where the geometry is discontinuous and these are regions where maximum values strongly depend on the mesh density. The peak values occurs already when the initial conditions are applied (swelling pressure and pore pressure) and are assumed to not cause any severe damage since they mainly are in a compressive state. Besides the singular regions the highest value occurs at the mid shell, 6.7% at 5 cm rock shearing magnitude when low friction is used for the fracture surface and 12.7% at 10 cm rock shearing magnitude when high friction is used for the fracture surface.

The peak value occurs for 10 cm shearing and are of course lower for the design case (5 cm shearing).

For the long term analyses the highest value of creep strain (CEEQ) occurs again at regions where the geometry is discontinuous, 17.7% (22% at 45 MPa) at 5 cm rock shearing magnitude and 19% respectively 28% at 10 cm rock shearing magnitude. At the mid shell the highest value is 7.2% (7.0 at 45 MPa) at 5 cm rock shearing magnitude and 17.7% (17.9% at 45 MPa) but if the buffer is removed the value is 14.5% already after 36 days, see Figures A3-13 to A3-25.

For the long term analyses the highest value of creep strain (CEEQ) occurs again at regions where the geometry is discontinuous (19%) and 2.1% at the top fillet but if the buffer is removed the value 13.8% is reached already after 36 days where the analysis stopped, see Figure A3-25.

8.2 Output regions

The numbers in Tables 8-2 to 8-5 and 8-8 to 8-11 are given for nine regions in the copper shell, see Figure 8-1 and should be used with care and in combination with the corresponding plots in the enclosed appendixes.

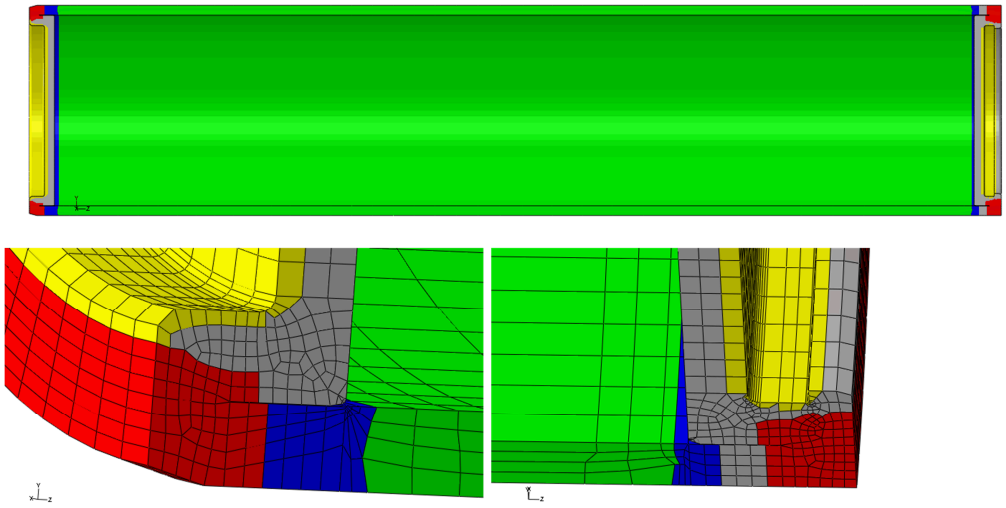

Figure 8-1*. Output regions for the copper shell. Region 1 - mid canister (green). Region 2 – top weld (red, lower right). Region 3 – base weld (red, lower left). Region 4 – top discontinuous geometry (blue, lower right). Region 5 – base discontinuous geometry (blue, lower left). Region 6 – top fillet (yellow, lower right). Region 7 – base fillet (yellow, lower left). Region 8 – top reminding (grey, lower right). Region 9 – base reminding (grey, lower left).*

Table 8-1. Summary of results for the insert and steel channel tubes.

Model name Model7_xx	1 – iron insert 2 – steel channel tubes	PEEQ/CEEQ [%]				Mises [MPa]				S33 [MPa] maximum tension		Comment
	Shearing [cm]	5		10		5		10		5	10	
	Insert material	1	2	1	2	1	2	1	2	1	1	
normal_third_2050ca3		0.5	0.9	1.9	2.1	399	565	435	579	148	187	Stopped at 8.7cm
normal_third_highfriction_2050ca3		0.8	1.3	2.2	3.2	404	560	460	605	258	278	
normal_third_creep_2050ca3		1.5	2.3	5.8	8.0	437	546	477	710	201	318	

Table 8-2. Summary of strain results for the copper shell at 5 cm shearing.

Model name Model7_xx	1 – mid shell 2,3 – top/base welds 4,5 – top/base discontinuous 6,7 – top/base fillets 8,9 – top/base reminding	PEEQ/CEEQ [%]								
	Copper shell region	1	2	3	4	5	6	7	8	9
normal_third_2050ca3		6.7	4.5	4	2.3	16	1.8	0.1	5.4	1.4
normal_third_highfriction_2050ca3		5.6	4.1	2.2	2.3	17	2.4	1.15	8.3	0.9
normal_third_creep_2050ca3		6.8	7.5	6.9	1.8	4.9	0.5	0	0.4	0.4

Table 8-3. Summary of strain results for the copper shell at 10 cm shearing.

Model name Model7_xx	1 – mid shell 2,3 – top/base welds 4,5 – top/base discontinuous 6,7 – top/base fillets 8,9 – top/base reminding	PEEQ/CEEQ [%]								
	Copper shell region	1	2	3	4	5	6	7	8	9
normal_third_2050ca3		12.2	8.9	4.8	2.6	19.3	2.5	0.4	6.7	1.7
normal_third_highfriction_2050ca3		12.7	8.8	2.4	2.6	19.1	4.4	0.3	7.0	1.2
normal_third_creep_2050ca3		17.2	12	9.3	2.0	10.5	1.0	0.1	2.2	0.8

Table 8-4. Summary of stress results for the copper shell at 5 cm shearing.

Model name **Model7_xx**	**1 – mid shell** **2,3 – top/base welds** **4,5 – top/base discontinuous** **6,7 – top/base fillets** **8,9 – top/base reminding**	**Mises [MPa]**								
	Copper shell region	1	2	3	4	5	6	7	8	9
normal_third_2050ca3		172	104	127	121	194	97	84	138	93
normal_third_highfriction_2050ca3		161	104	127	125	200	105	81	136	100
normal_third_creep_2050ca3		325	257	172	332	332	221	163	294	182

Table 8-5. Summary of stress results for the copper shell at 10 cm shearing.

Model name **Model7_xx**	**1 – mid shell** **2,3 – top/base welds** **4,5 – top/base discontinuous** **6,7 – top/base fillets** **8,9 – top/base reminding**	**Mises [MPa]**								
	Copper shell region	1	2	3	4	5	6	7	8	9
normal_third_2050ca3		213	117	106	114	194	106	88	155	108
normal_third_highfriction_2050ca3		216	119	92	114	201	128	83	158	96
normal_third_creep_2050ca3		344	242	241	231	336	225	241	287	264

Table 8-6. Summary of results (insert and steel channel tubes) for long term rock shear analyses after 5 cm shearing.

Model name Model7_xx	1 – iron insert 2 – steel channel tubes	PEEQ/CEEQ [%]		Mises [MPa]		S33 [MPa] maximum tension
	Insert material	1	2	1	2	1
normal_third_creep1_relax_2050ca3		1.9	2.6	442	522	199
normal_third_creep1_45_relax_2050ca3		3.2	4.8	443	611	207

Table 8-7. Summary of results (insert and steel channel tubes) for long term rock shear analyses after 10 cm shearing.

Model name Model7_xx	1 – iron insert 2 – steel channel tubes	PEEQ/CEEQ [%]		Mises [MPa]		S33 [MPa] maximum tension	Comment
	Insert material	1	2	1	2	1	
normal_third_creep_relax_2050ca3		6.0	0.4	437	370	244	
normal_third_creep1_2050ca3_r2		5.0	6.6	465	684	234	Stopped after 36 days
normal_third_creep_45_relax_2050ca3		7.5	11	459	730	331	

Since the creep model also contains plastic deformation the main part of creep strains are reached already at the shearing phase (after 0.1 second). Thereafter only small changes of the creep strains are observed.

The creep strain after long time (100,000 years) shows similar behavior for all listed results – the strains (CEEQ/PEEQ) increases with time and the stresses decreases, compare Tables 8-1 to 8-5 with Tables 8-8 to 8-11.

Maximum creep strain is 17.9% (neglecting singular regions) compared to 12.7% when elastic-plastic material is used at 10 cm shearing (low friction), see Tables 8-3 and 8-9.

Mises' stress relaxes linearly with time in a lin-log diagram, see Appendix 3.

Table 8-8. Summary of strain results in the copper shell for long term rock shear analyses after 5 cm shearing.

Model name Model7_xx	1 – mid shell 2,3 – top/base welds 4,5 – top/base discontinuous 6,7 – top/base fillets 8,9 – top/base reminding	PEEQ/CEEQ [%]								
	Copper shell region	1	2	3	4	5	6	7	8	9
normal_third_creep1_relax_2050ca3		7.2	7.6	6.9	3.3	17.7	1.4	0.1	2.5	1.4
normal_third_creep1_45_relax_2050ca3		7.0	7.8	7.0	4.9	22	1.9	0.1	4.8	2.1

Table 8-9. Summary of strain results in the copper shell for long term rock shear analyses after 10 cm shearing.

Model name Model7_xx	1 – mid shell 2,3 – top/base welds 4,5 – top/base discontinuous 6,7 – top/base fillets 8,9 – top/base reminding	PEEQ/CEEQ [%]								
	Copper shell region	1	2	3	4	5	6	7	8	9
normal_third_creep_relax_2050ca3		17.7	12.0	9.3	3.0	19	2.1	0.5	7.6	1.8
normal_third_creep1_2050ca3_r2		14.5	9.0	7.7	3.1	16.5	13.8	13.2	3.1	1.3
normal_third_creep_45_relax_2050ca3		17.9	12.2	9.6	4.7	28	2.3	0.4	6.1	2.5

Table 8-10. Summary of stress results in the copper shell for long term rock shear analyses after 5 cm shearing.

Model name Model7_xx	1 – mid shell 2,3 – top/base welds 4,5 – top/base discontinuous 6,7 – top/base fillets 8,9 – top/base reminding	Mises [MPa]								
	Copper shell region	1	2	3	4	5	6	7	8	9
normal_third_creep1_relax_2050ca3		184	162	138	166	232	147	131	138	139
normal_third_creep1_45_relax_2050ca3		192	217	207	157	249	167	130	159	168

Table 8-11. Summary of stress results in the copper shell for long term rock shear analyses after 10 cm shearing.

Model name Model7_xx	1 – mid shell 2,3 – top/base welds 4,5 – top/base discontinuous 6,7 – top/base fillets 8,9 – top/base reminding	Mises [MPa]								
	Copper shell region	1	2	3	4	5	6	7	8	9
normal_third_creep_relax_2050ca3		212	234	159	136	238	158	137	167	144
normal_third_creep1_2050ca3_r2		258	203	176	191	248	320	313	308	298
normal_third_creep_45_relax_2050ca3		214	250	231	153	266	161	137	163	186

9 Uncertainties

The obtained results are based on several assumptions regarding loads and material properties. Also the discretization in the computer model will affect the results. Some of these influencing factors are addressed below.

- Strain rate effects for bentonite, copper and iron will affect the results. Copper canister will have the strain rate effect included when the creep model is used but not for analyzes performed by using plasticity theory. The comparison, see Tables 8-1 to 8-5, indicate that the creep model will increase the maximum strain and stress level.

- The coefficient of friction at fracture surface is unknown but the results (Tables 8-1 to 8-5), indicate that increasing the coefficient of friction will slightly increase the maximum strain and stress level.

- All experiments used for material calibration have a spread which will imply a range for the properties defining each material model.

- Swelling pressure for the bentonite will affect the material stiffness. The experimental results have a spread in the results and the used data should be conservative in the sense that the obtained stress and strain magnitudes are overestimated.

- Element mesh is rather fine but nevertheless it is too coarse in some regions, especially at the welds and regions with geometric discontinuities. A more refined mesh will probably increase the maximum stress and strain levels. Fortunately, the use of non-linear material properties (such as plasticity and creep) will decrease the sensitivity to the used mesh. The used mesh has been judged to be accurate enough considering also the required computer resources to obtain the results. Since several models have been executed with different mesh densities it has been possible to compare and the conclusion is that the mesh in a global sense is accurate.

- The creep analysis has been performed at 27 ^{o}C but the material model for the insert has experimental results for 0 ^{o}C. It is assumed that the properties are accurate enough but this has not so far been checked.

10 Evaluation and conclusion

The results obtained from the rock shear analyses could be summarized as:

- Two different approached have been used when simulating the impact from the glacial, none of these are perfect:
    - Removing the buffer implies that the stabilizing effect from the buffer is lost
    - Keeping the buffer will distribute the added load in a not correct way
    - Most accurate is to use elements with pore-pressure as a degree of freedom but a calibrated material model for this case is not available
    - Another reasonable alternative is to start the analysis with a total hydrostatic pressure of 45 MPa followed by a creep analysis for the time period of the glacial.
- The maximum plastic strain in the copper canister occurs in fillets (besides regions containing singularities) but also the global level close to the fracture surface in the canister shows high plastic strains. When the copper canister is modeled with creep included the highest creep strain occurs at the global level and without any buffer the creep strain increases quickly.
- When the hydrostatic pressure is increased from 15 to 45 MPa the plastic strains increase further. However, the obtained strains in the copper shell are still below the level causing any failure (the experiments are done up to about 50% strain, Figure 3-4, which is substantially greater than the calculated maximum strain (17.9%).
- Maximum principal stress in the insert mainly comes from bending of the canister – the level depends mainly on material properties for the insert (and dimensions) and buffer stiffness.
- Creep doesn't seem to be a major concern (if the buffer is active) since the copper deformation is controlled by the surrounding material which implies small creep strain rates as soon as the final deformation has been established. Also the bentonite will have some creep (has not been considered) which will lower the stress level in the copper and thus contribute to less creep in the copper.
- Maximum creep strain (CEEQ) differs to maximum plastic strain (PEEQ) when comparing elastic-plastic and creep models and the model giving the highest strain depends on region.

11 References

SKB's (Svensk Kärnbränslehantering AB) publications can be found at www.skb.se/publications. References to SKB's unpublished documents are listed separately at the end of the reference list. Unpublished documents will be submitted upon request to document@skb.se.

ABAQUS, 2008. Version 6.10.1. Dassault Systèmes Simulia Corp.

Andersson-Östling H C M, Sandström R, 2009. Survey of creep properties intended for nuclear waste disposal. SKB TR-09-32, Svensk Kärnbränslehantering AB.

Börgesson L, Johannesson L-E, Hernelind J, 2004. Earthquake induced rock shear through a deposition hole. Effect on the canister and the buffer. SKB TR-04-02, Svensk Kärnbränslehantering AB.

Börgesson L, Johannesson L-E, Sandén T, Hernelind J, 1995. Modelling of the physical behavior of water saturated clay barriers. Laboratory tests, material models and finite element application. SKB TR-95-20, Svensk Kärnbränslehantering AB.

Börgesson L, Dueck A, Johannesson L-E, 2010. Material model for shear of the buffer – evaluation of laboratory test results. SKB TR-10-31, Svensk Kärnbränslehantering AB.

Hernelind J, 2010. Modelling and analysis of canister and buffer for earthquake induced rock shear and glacial. SKB TR-10-34, Svensk Kärnbränslehantering AB.

Jin L-Z, Sandström R, 2008. Creep of copper canisters in power-law breakdown. Computational Materials Science, 43, 403–416**.**

Raikko H, Sandström R, Rydén H, Johansson M, 2010. Design analysis report for the canister. SKB TR-10-28, Svensk Kärnbränslehantering AB.

Sandström R, Andersson H C M, 2008. Creep in phosphorus alloyed copper during power-law breakdown. Journal of Nuclear Materials, 372, 76-88.

Sandström R, Hallgren J, Burman G, 2009. Stress strain flow curves for Cu-OFP. SKB R-09-14, Svensk Kärnbränslehantering AB.

SKB, 2009, Design Premises for a KBS-3V repository based on results from safety assessment SR-Can and some subsequent analyses. SKB TR-09-22, Svensk Kärnbränslehantering AB.

SSABDirekt, 2008. Steelfacts Domex 355 MC. Available at http://www.ssabdirect.com. [19 September 2008].

SS-EN 10025-2:2004. Varmvalsade konstruktionsstål – Del 2: Tekniska leveransbestämmelser för olegerade stål (Hot rolled products of structural steels - Part 2: Technical delivery conditions for non-alloy structural steels). Stockholm: Swedish Standards Institute.

Unpublished documents

SKBdoc id, version	Title	Issuer, year
1203875 ver 1.0	Ritningsförteckning för kapselkomponenter	SKB, 2009
1201865 ver 1.0	Dragprovning av gjutjärn	KTH, 2009
1339902 ver 1.0	Global simulation of copper canister-final deposition	SKB, 2014
1407337 ver 1.0	Earthquake induced rock shear through a deposition hole – part 2	SKB 2014

Revision audit trail

Version	Date	Description	Author	Reviewed	Approved
2.0	2014-03-14	Figures in Appendix 3 are revised, headlines no 1 starts on a new page in the entire report	Jan Hernelind/ 5T Engineering AB	as first pageheader	as first pageheader
1.0	2010-02-03	New report.	Jan Hernelind/5T Engineering AB	Sanja Trkulja (QA)	Jan Sarnet

Appendix 1 – Short term rock shear normal to canister axis at 2/3 from base of canister 2050ca3 (tension)

Plots showing deformed geometry, plastic strain (PEEQ), Mises stress (MISES) for shearing magnitudes 5 and 10 cm.

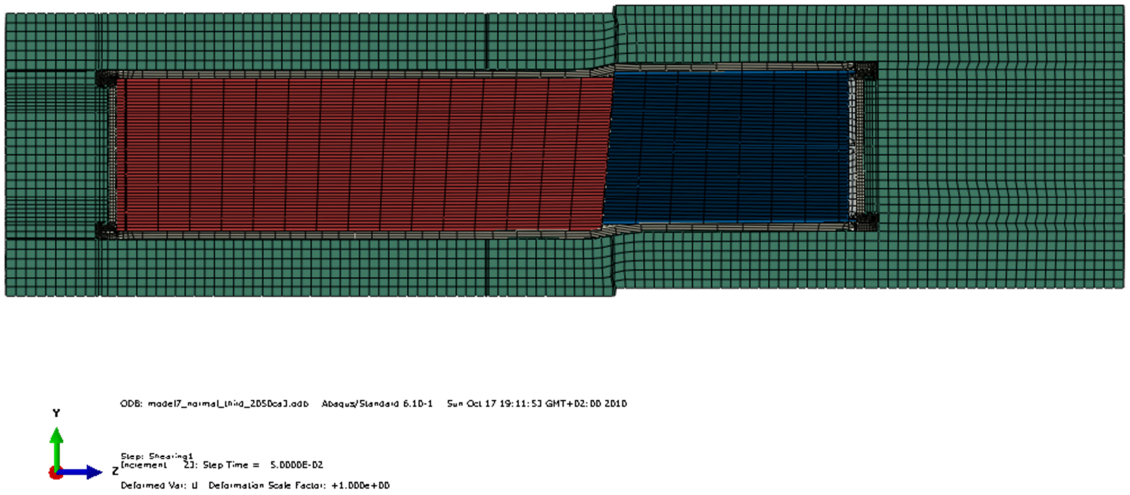

Figure A1-1. *Deformed geometry - 5 cm shearing magnitude.*

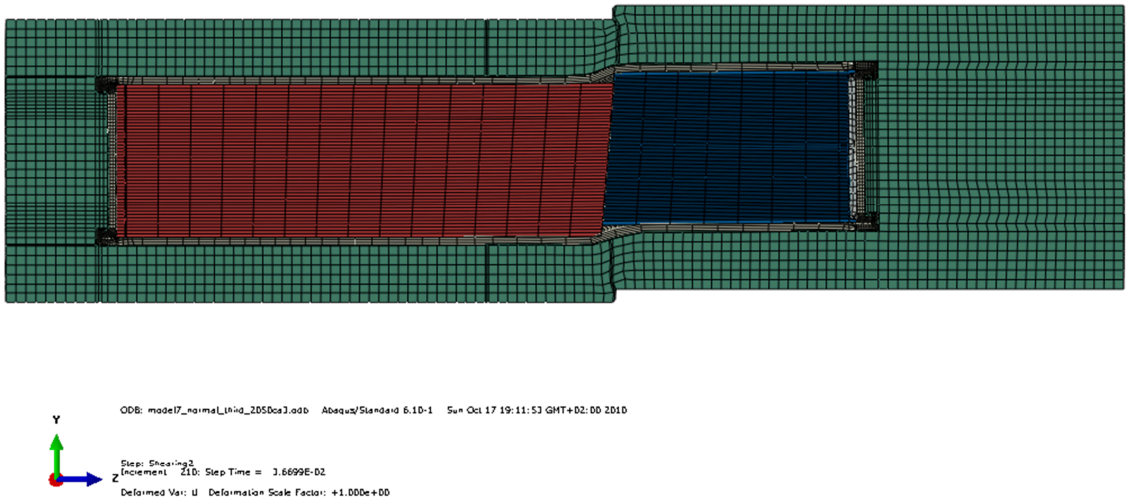

Figure A1-2. *Deformed geometry - 10 cm shearing magnitude.*

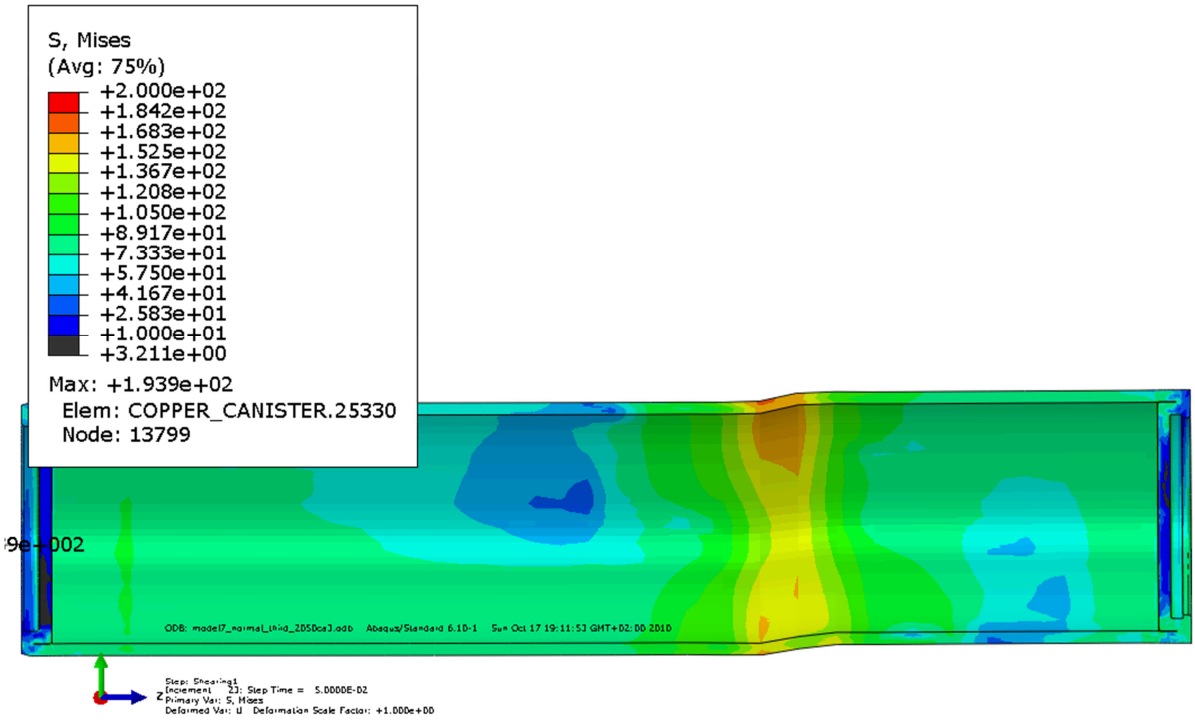

Figure A1-3*. Mises stress for copper shell - 5 cm shearing magnitude.*

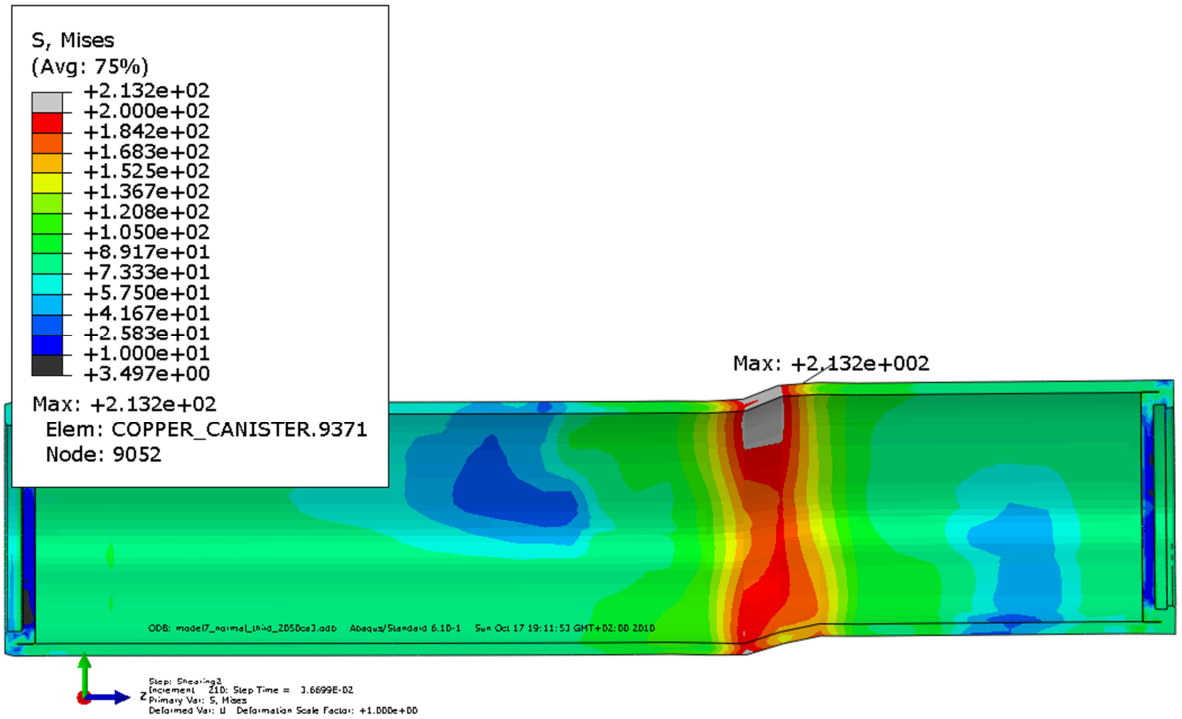

Figure A1-4. *Mises stress for copper shell - 10 cm shearing magnitude.*

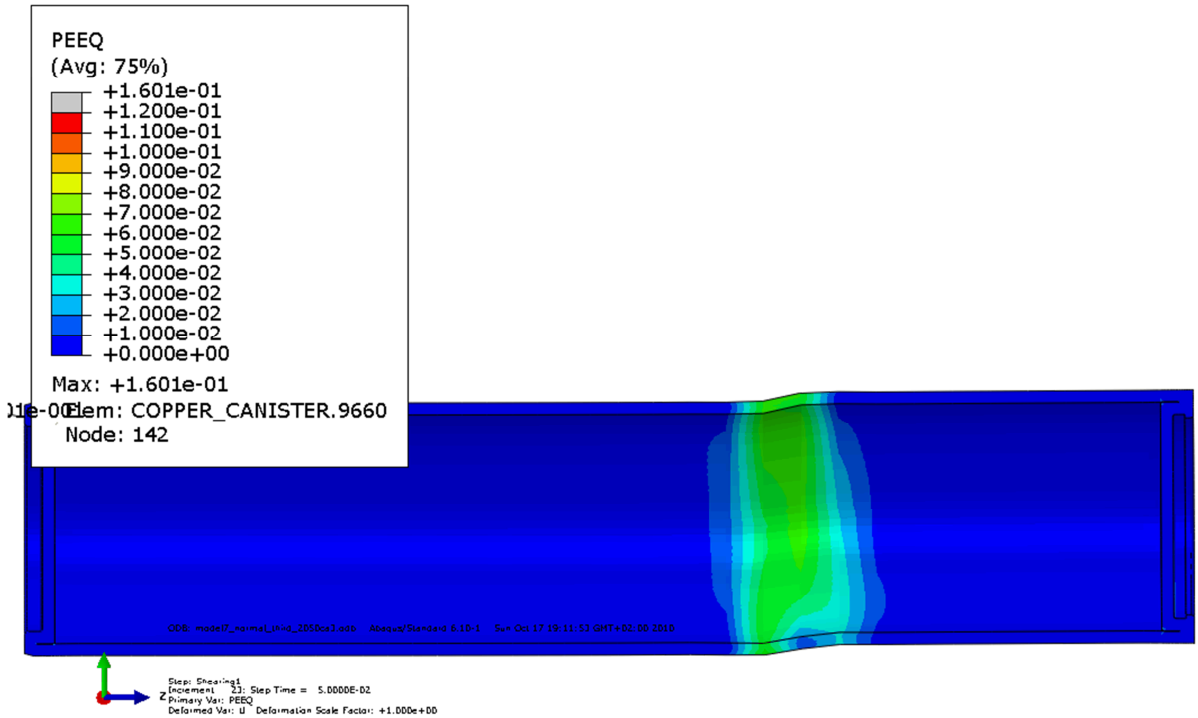

Figure A1-5. *Plastic strain (PEEQ) for copper shell - 5 cm shearing magnitude.*

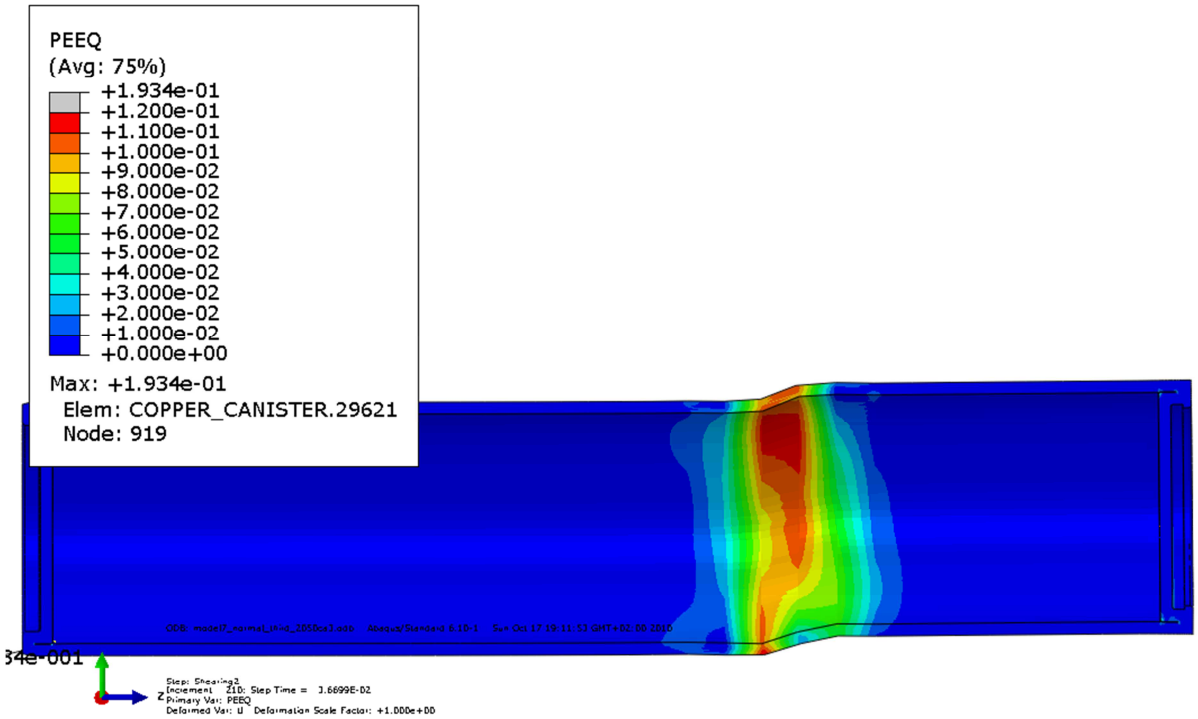

Figure A1-6. *Plastic strain (PEEQ) for copper shell - 10 cm shearing magnitude.*

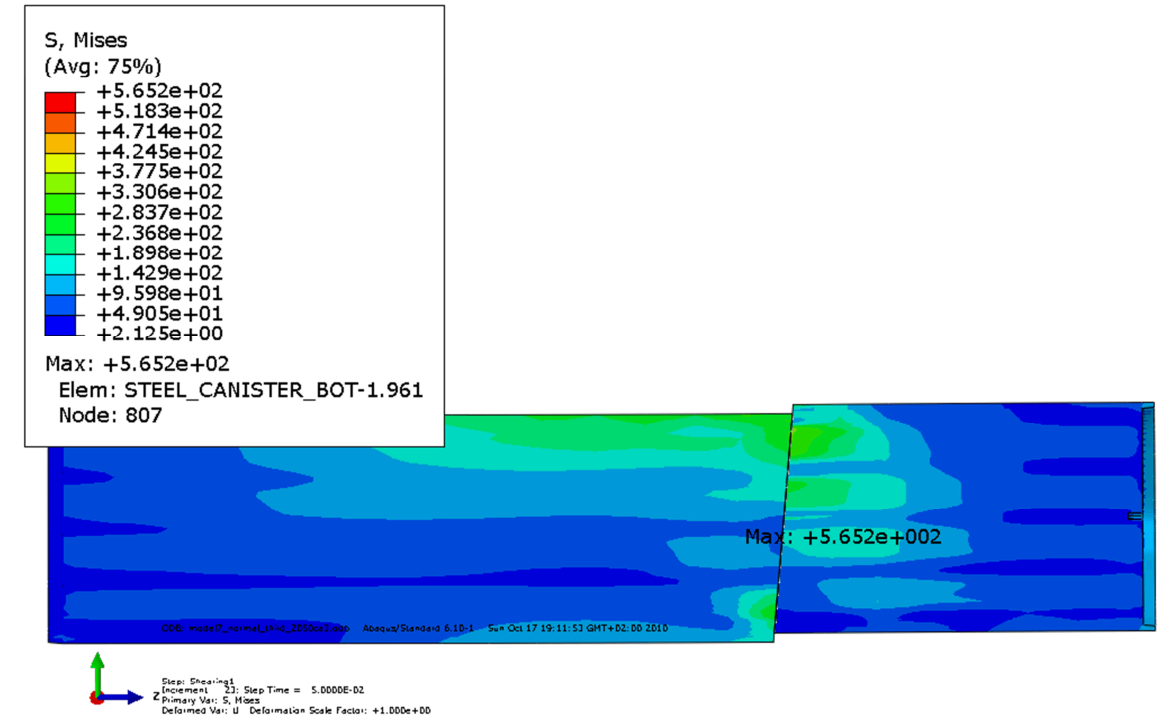

Figure A1-7. *Mises stress for insert - 5 cm shearing magnitude.*

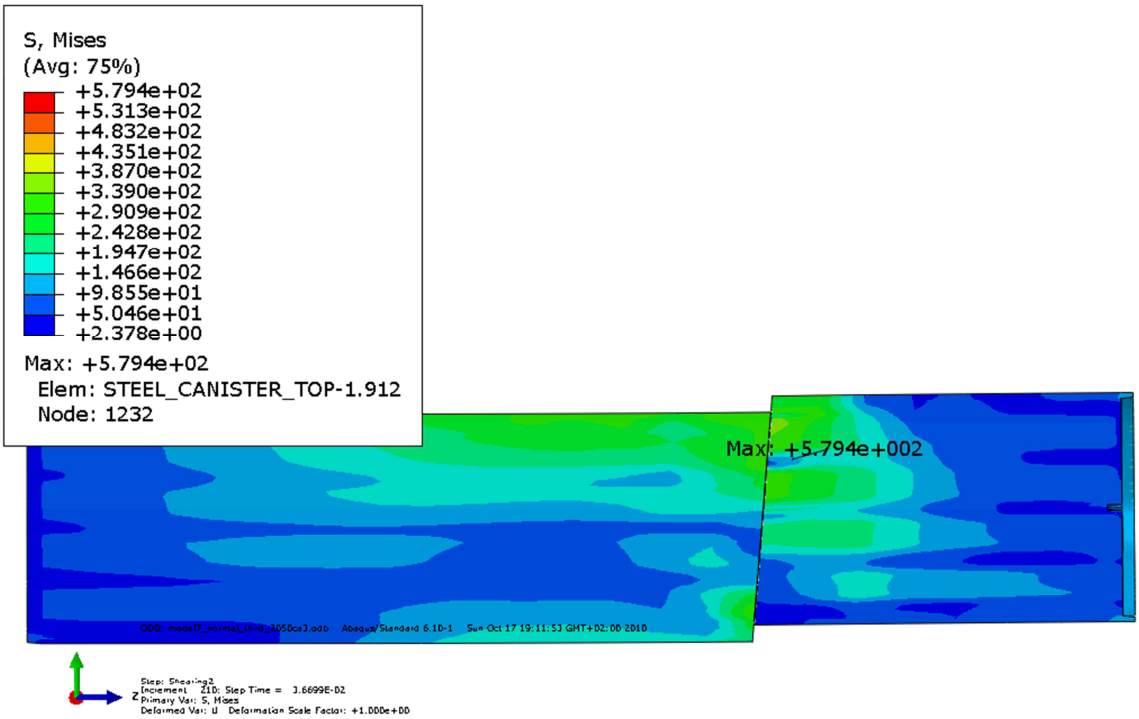

Figure A1-8. *Mises stress for insert - 10 cm shearing magnitude.*

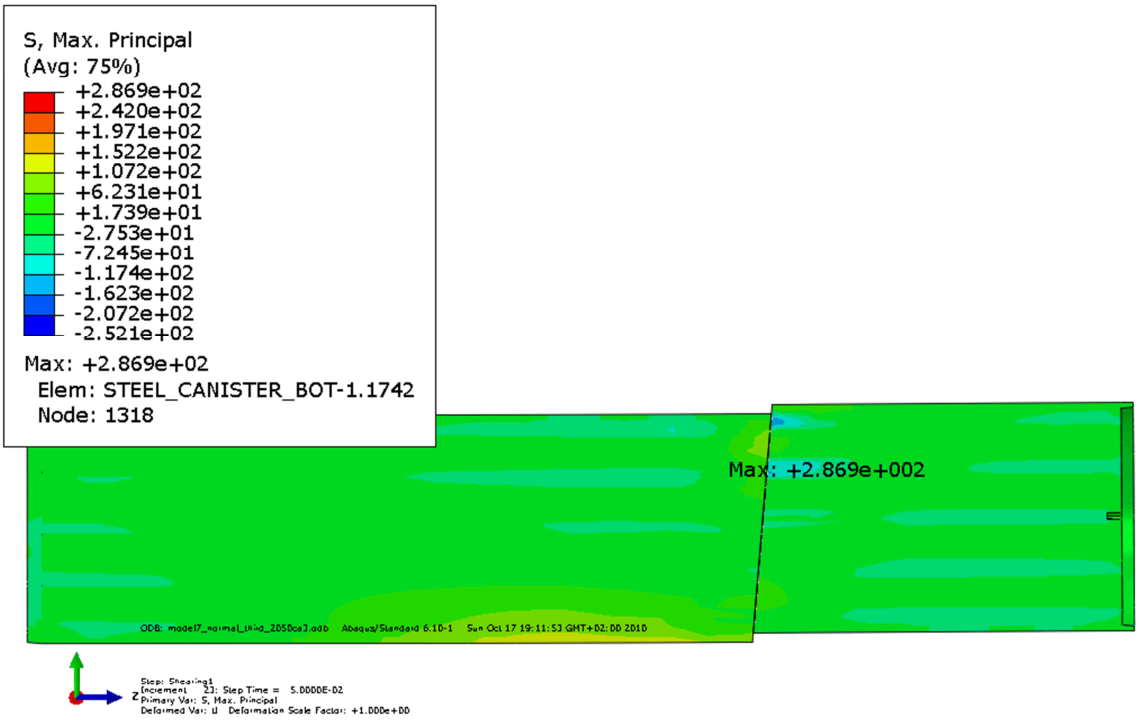

Figure A1-9. *Max principal stress for insert - 5 cm shearing magnitude.*

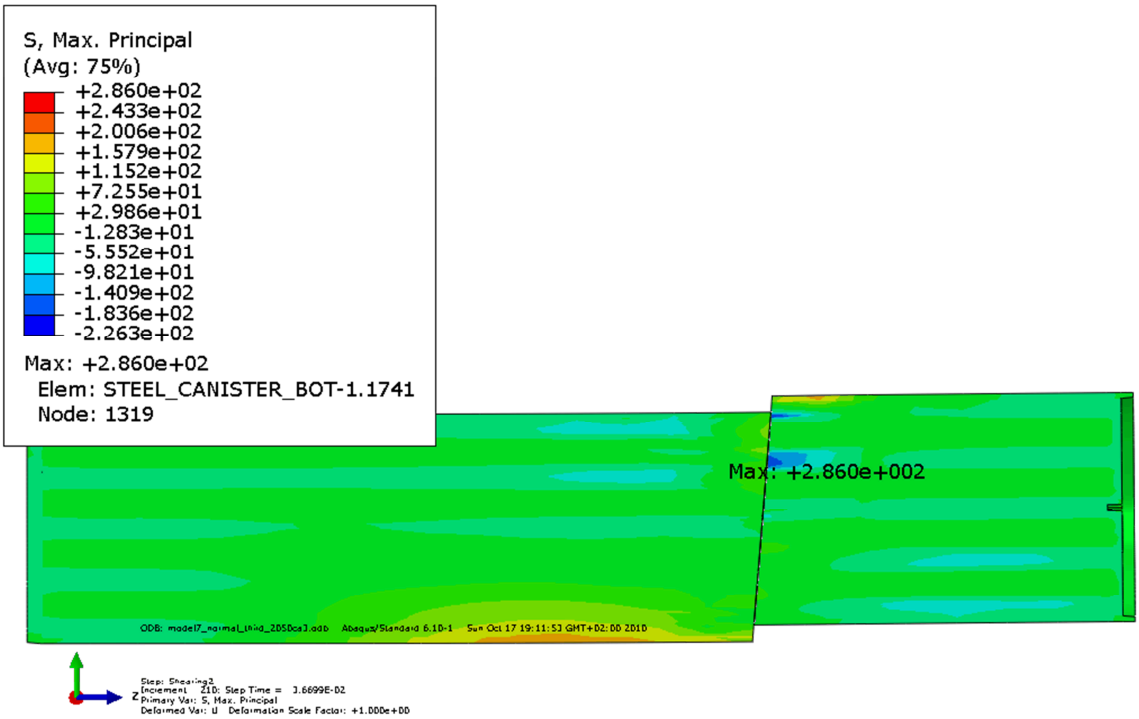

Figure A1-10. *Max principal stress for insert - 10 cm shearing magnitude.*

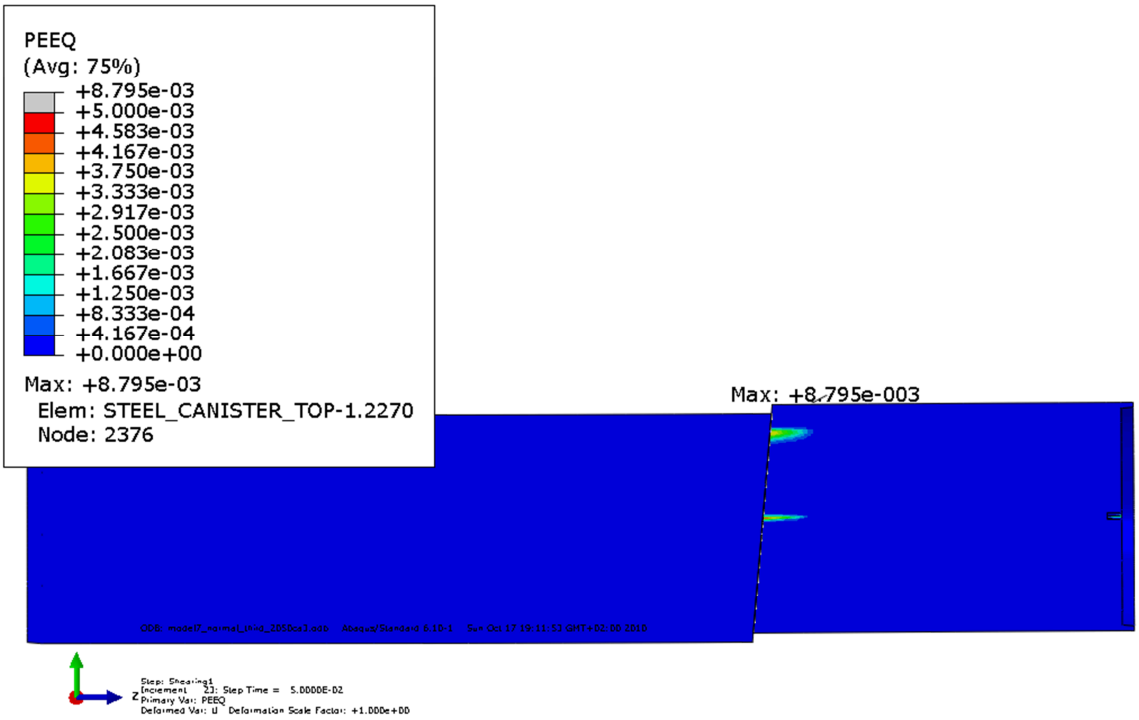

Figure A1-11. *Plastic strain (PEEQ) for insert - 5 cm shearing magnitude.*

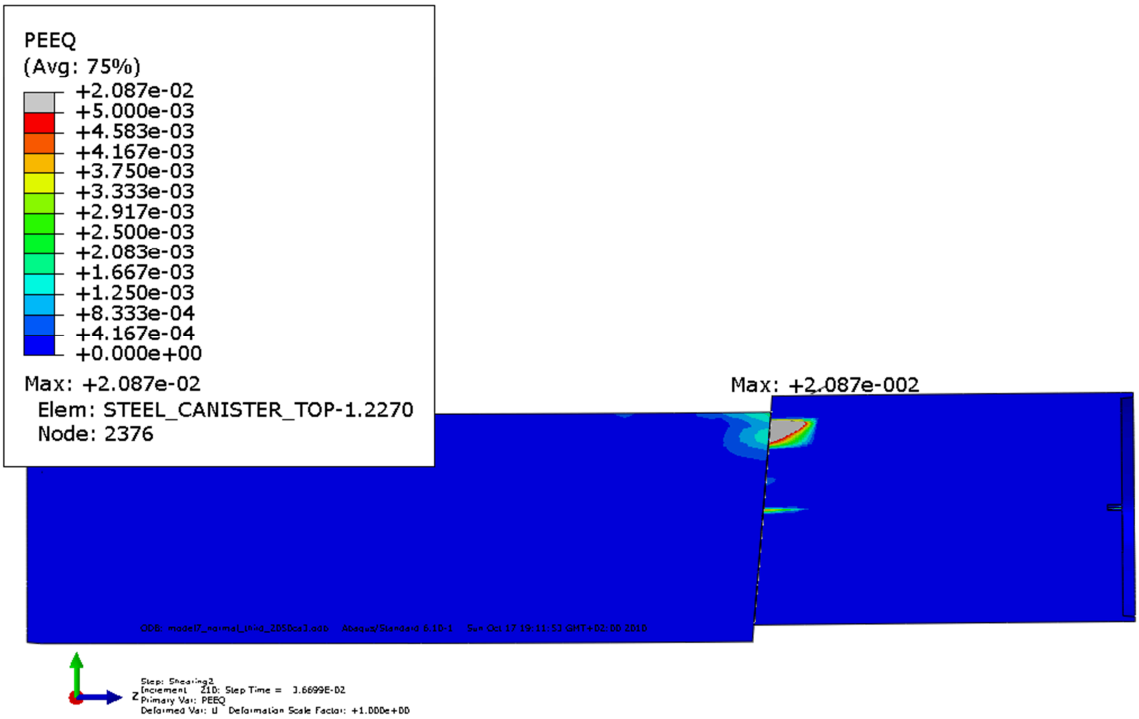

Figure A1-12. *Plastic strain (PEEQ) for insert - 10 cm shearing magnitude.*

Appendix 2 – Short term rock shear normal to canister axis at 2/3 from base of canister – high friction 2050ca3, tension

Plots showing deformed geometry, plastic strain (PEEQ), Mises stress (MISES) for shearing magnitudes 5 and 10 cm.

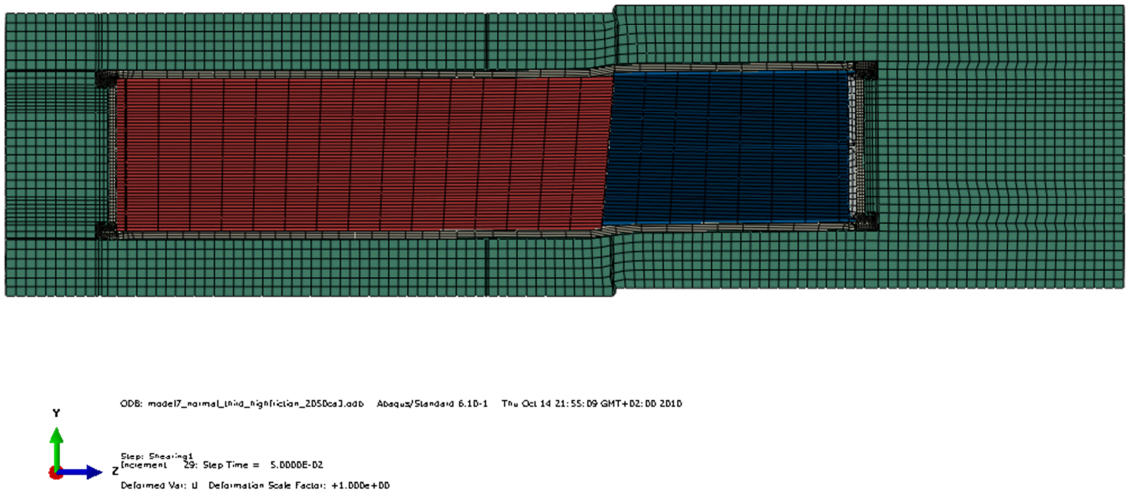

Figure A2-1. *Deformed geometry - 5 cm shearing magnitude.*

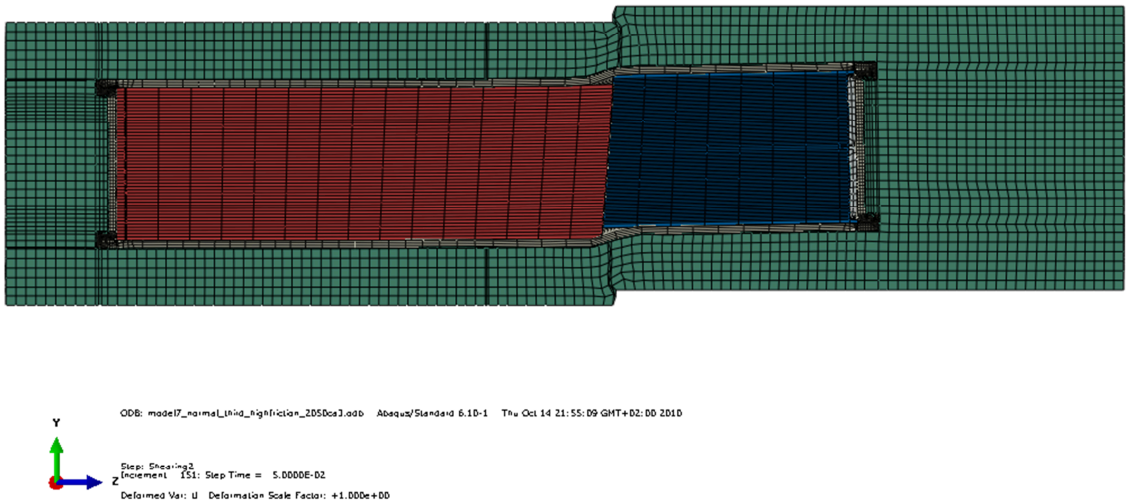

Figure A2-2. *Deformed geometry - 10 cm shearing magnitude.*

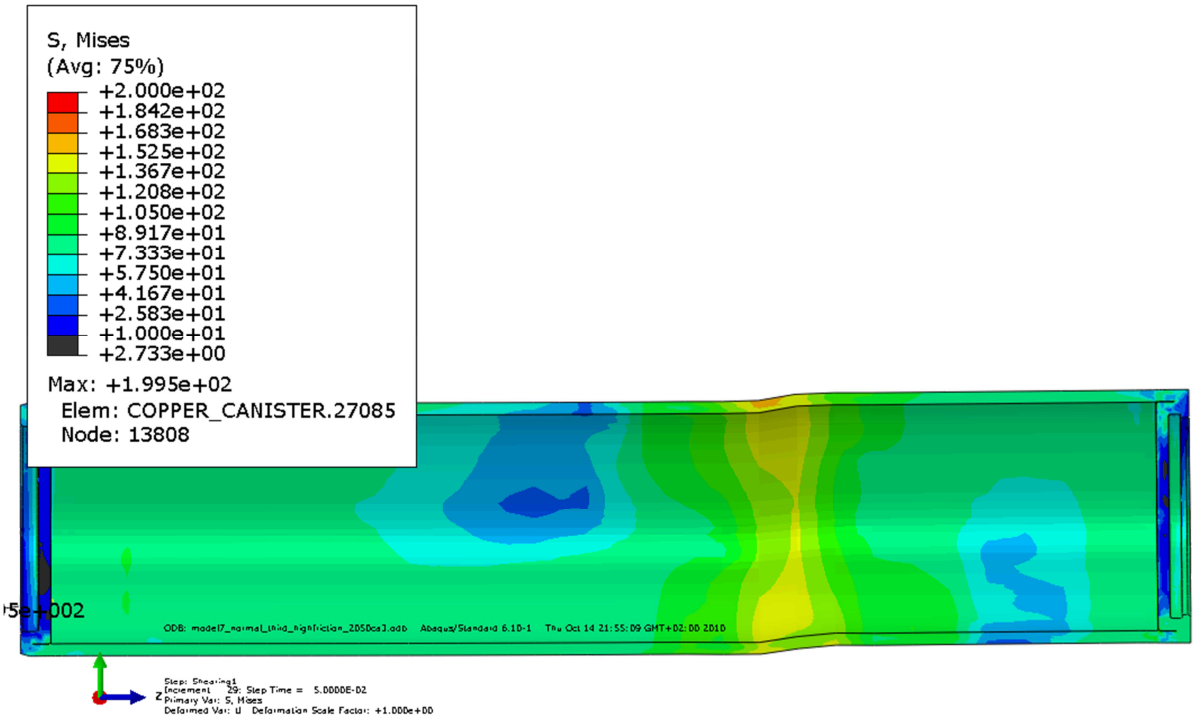

Figure A2-3. *Mises stress for copper shell - 5 cm shearing magnitude.*

.

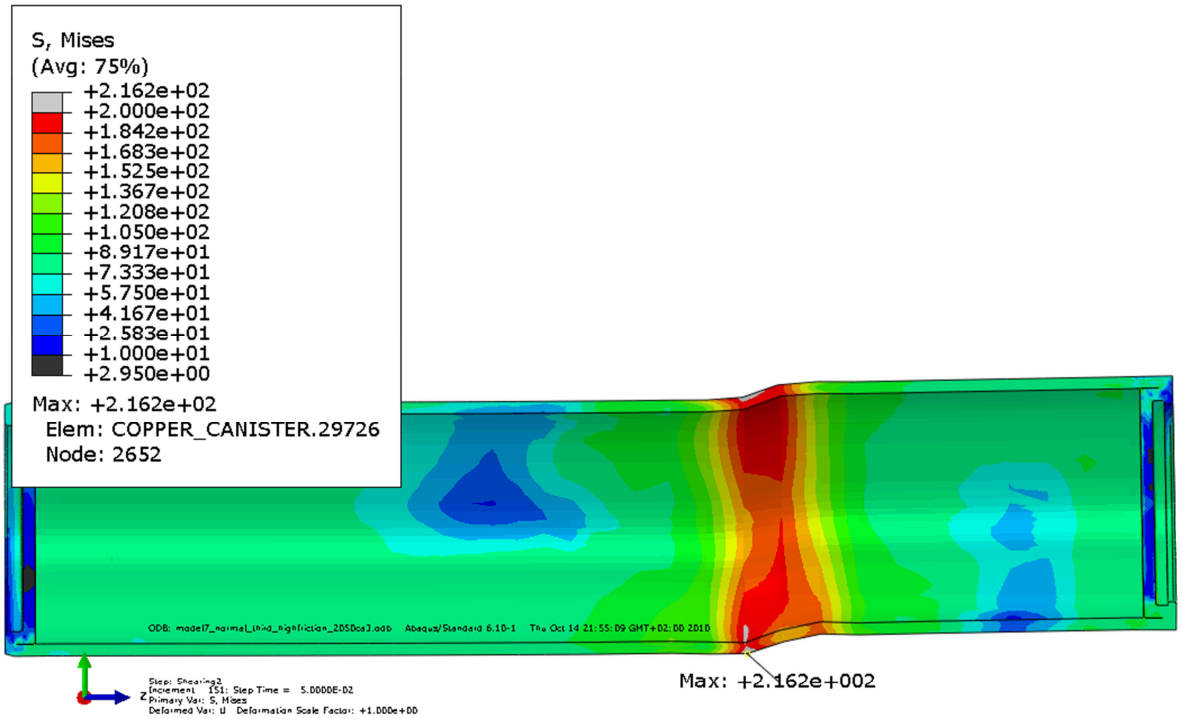

Figure A2-4. *Mises stress for copper shell - 10 cm shearing magnitude.*

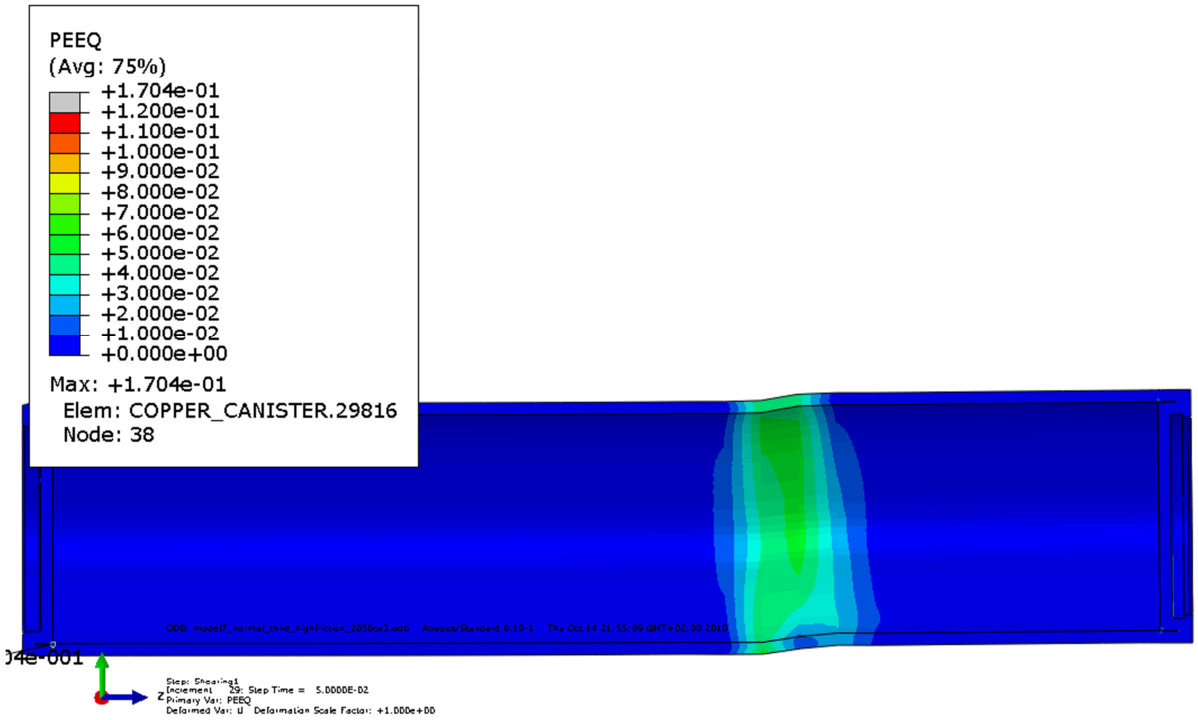

Figure A2-5. *Plastic strain (PEEQ) for copper shell - 5 cm shearing magnitude.*

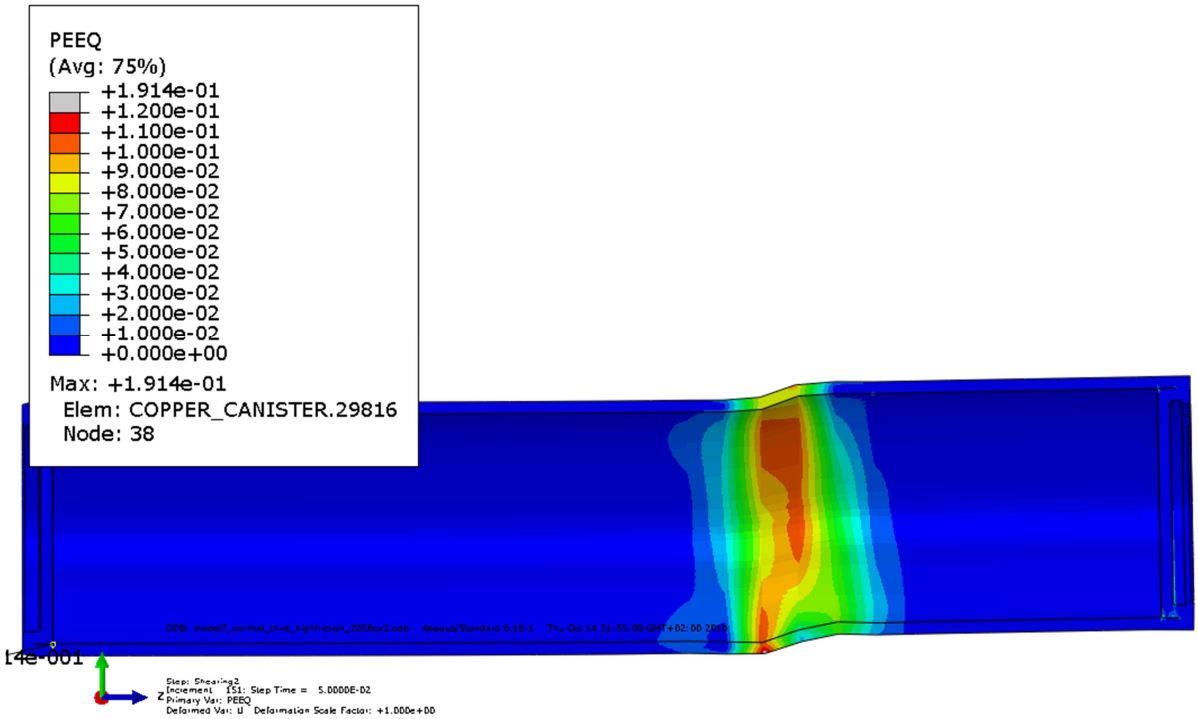

Figure A2-6. *Plastic strain (PEEQ) for copper shell - 10 cm shearing magnitude.*

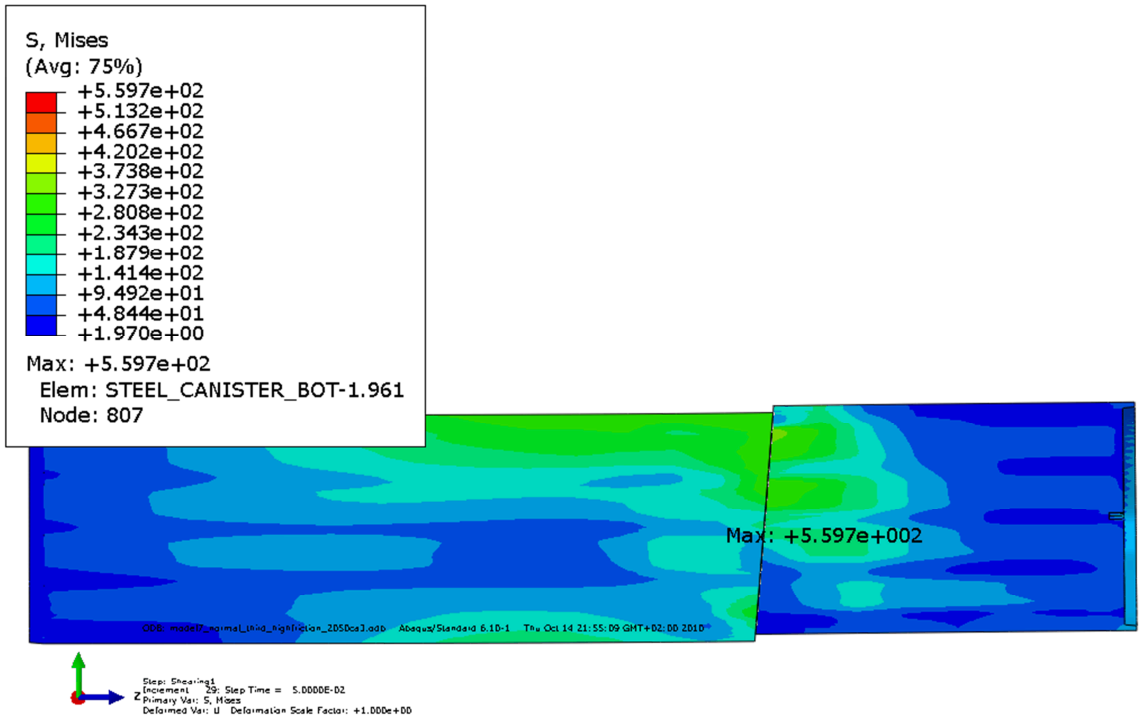

Figure A2-7. *Mises stress for insert - 5 cm shearing magnitude.*

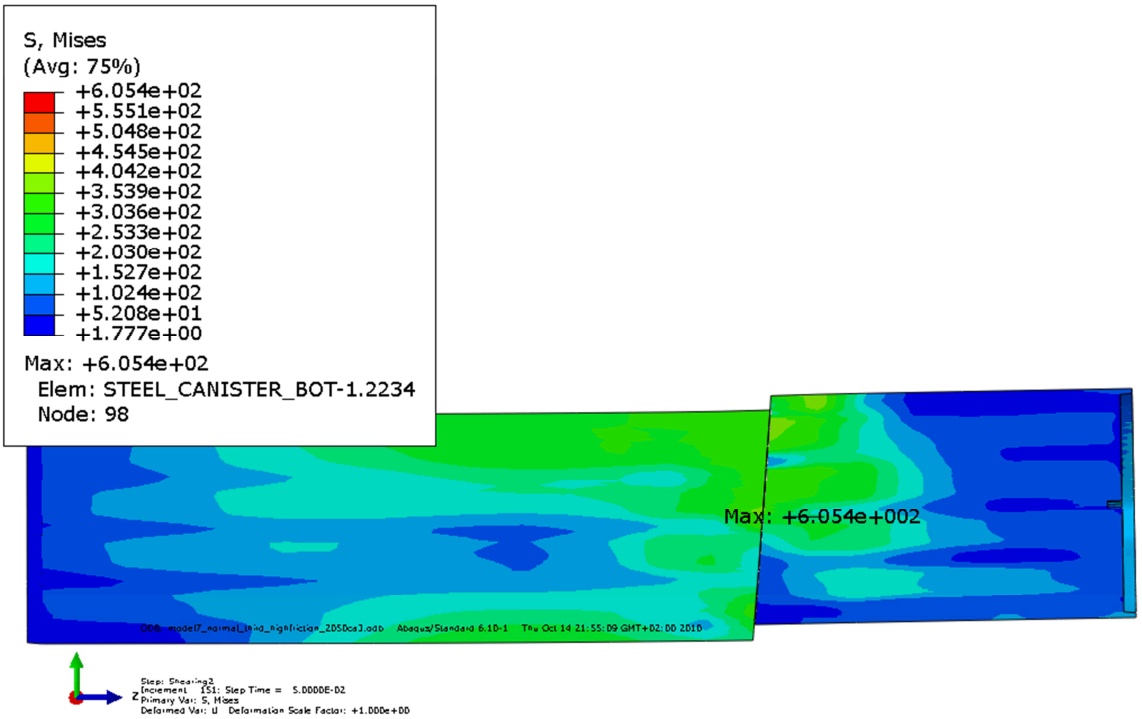

Figure A2-8. *Mises stress for insert - 10 cm shearing magnitude.*

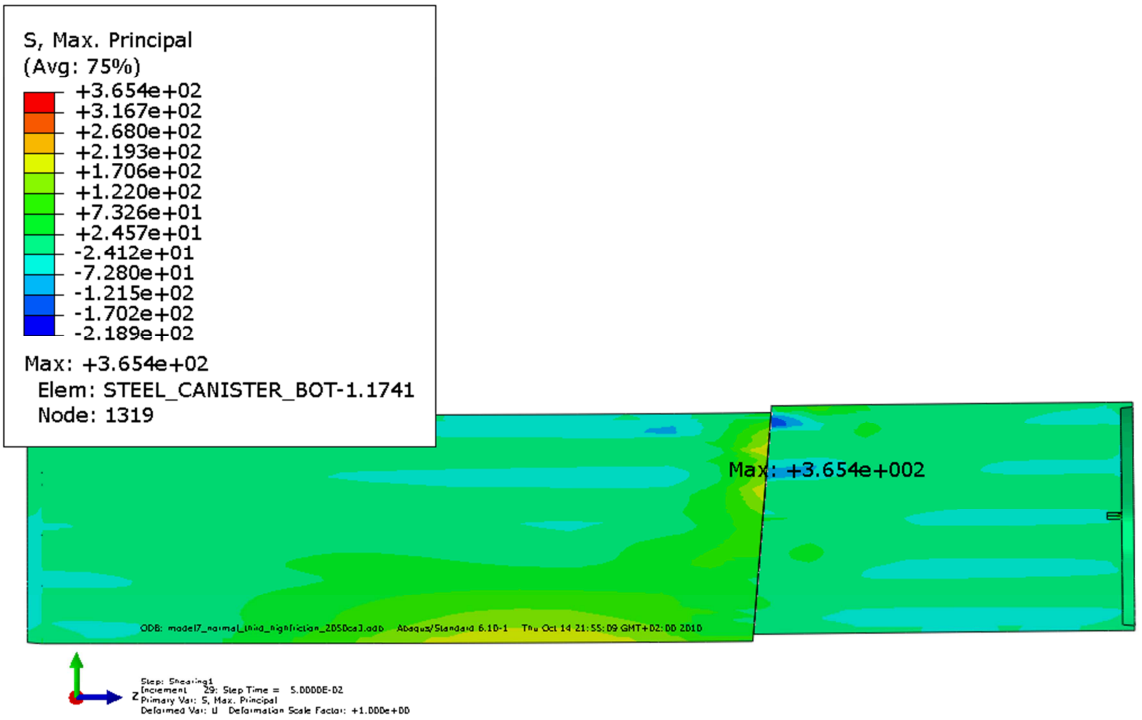

Figure A2-9. *Max principal stress for insert - 5 cm shearing magnitude.*

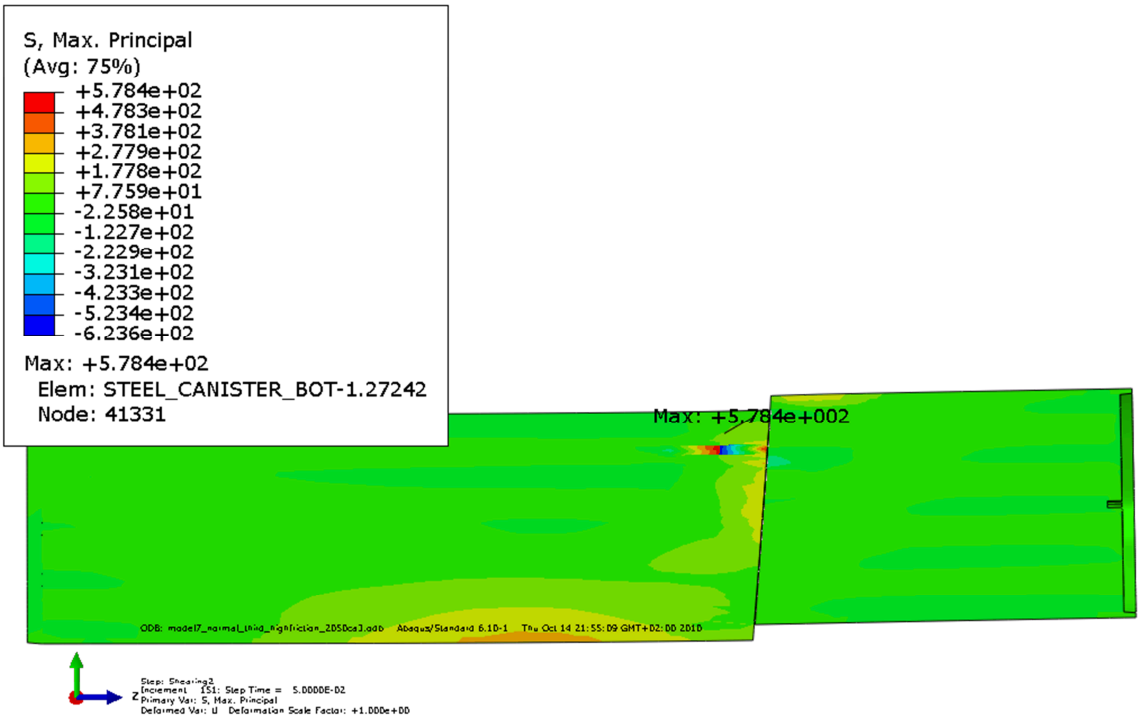

Figure A2-11. *Max principal stress for insert - 10 cm shearing magnitude.*

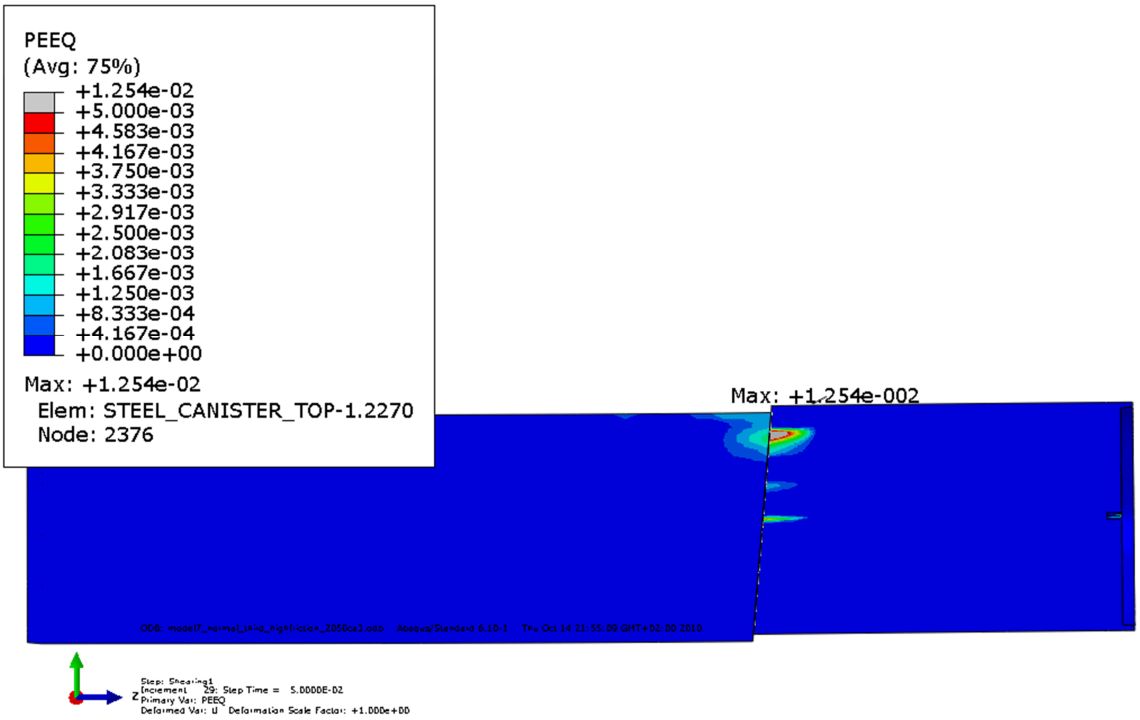

Figure A2-12. *Plastic strain (PEEQ) for insert - 5 cm shearing magnitude.*

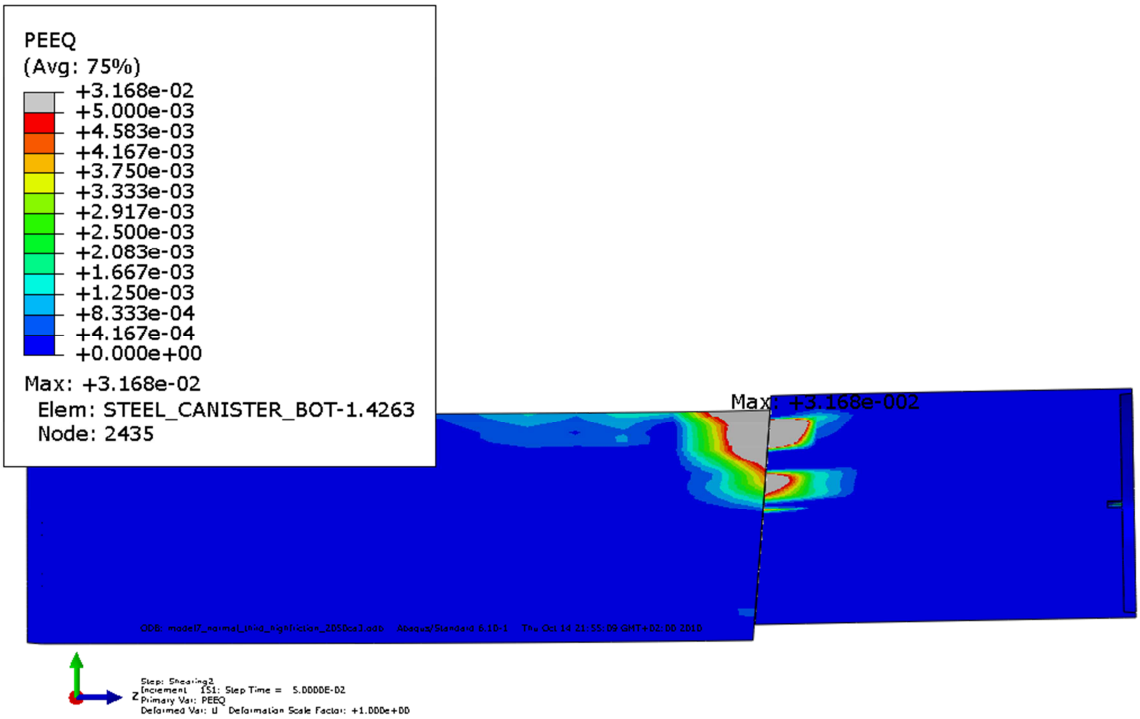

***Figure A2-13**. Plastic strain (PEEQ) for insert - 10 cm shearing magnitude.*

Appendix 3 – Long term rock shear normal to canister axis at 2/3 from base canister – 2050ca3 (tension)

Plots showing deformed geometry, plastic strain (CEEQ/PEEQ), Mises stress (MISES) for shearing magnitudes 5 and 10 cm. Note that for Figures A3-1 to A3-6 100% threshold has been used for averaging of nodal contributions and for the rest of the Figures the threshold value is 0%.

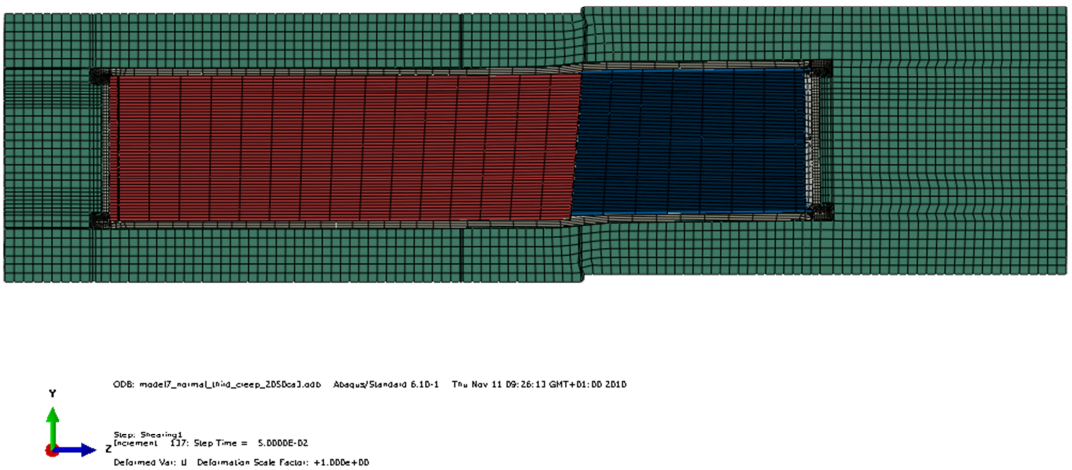

Figure A3-1. *Deformed geometry - 5 cm shearing magnitude.*

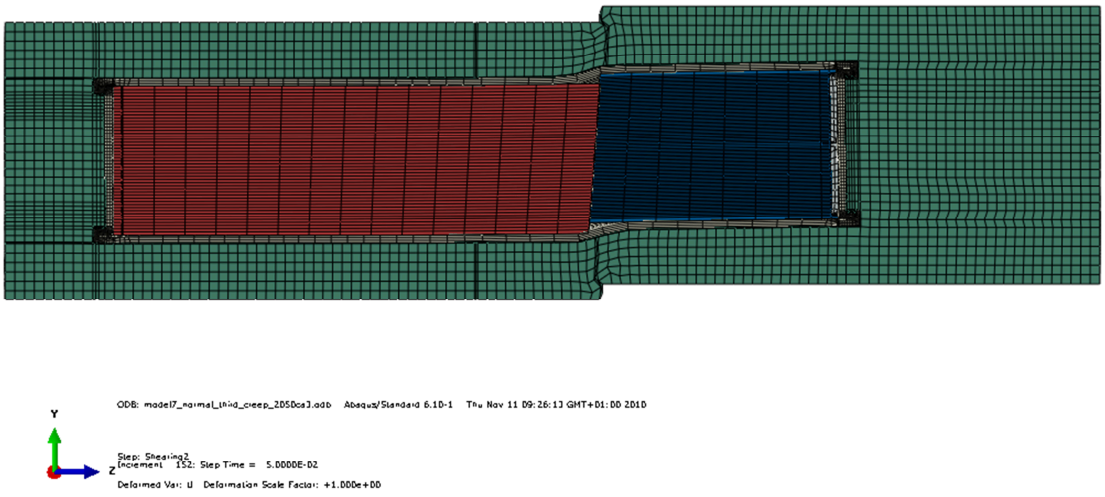

Figure A3-2. *Deformed geometry - 10 cm shearing magnitude.*

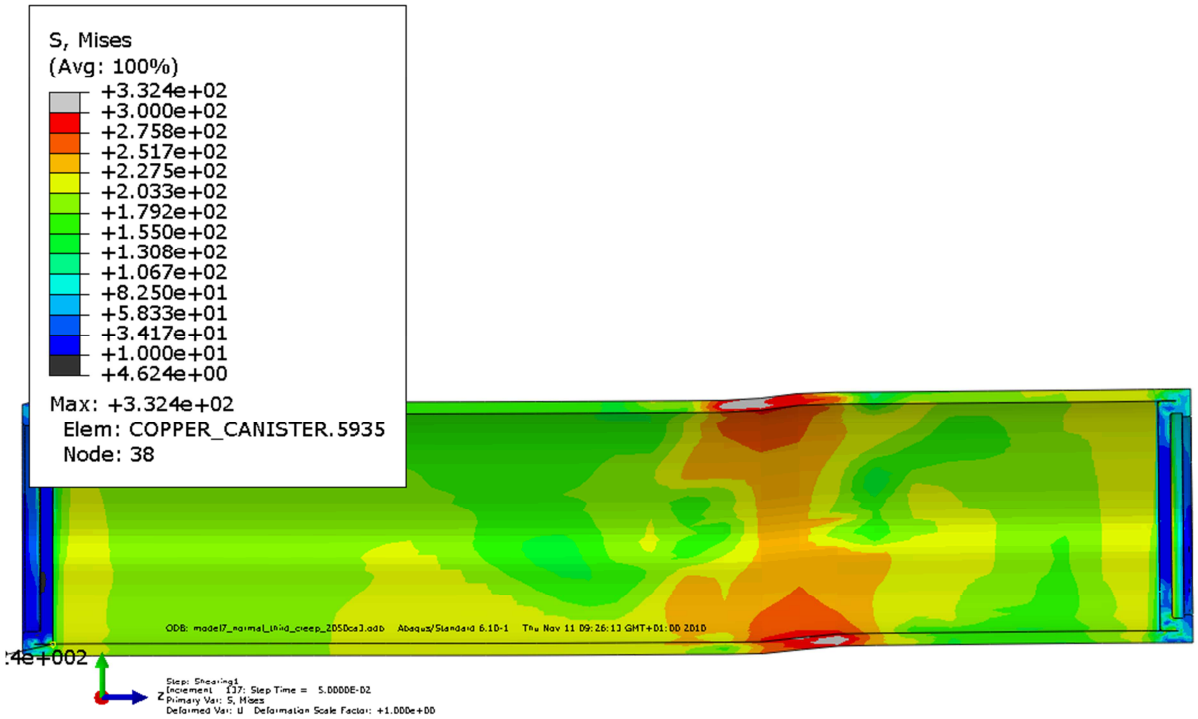

Figure A3-3. *Mises stress for copper shell - 5 cm shearing magnitude.*

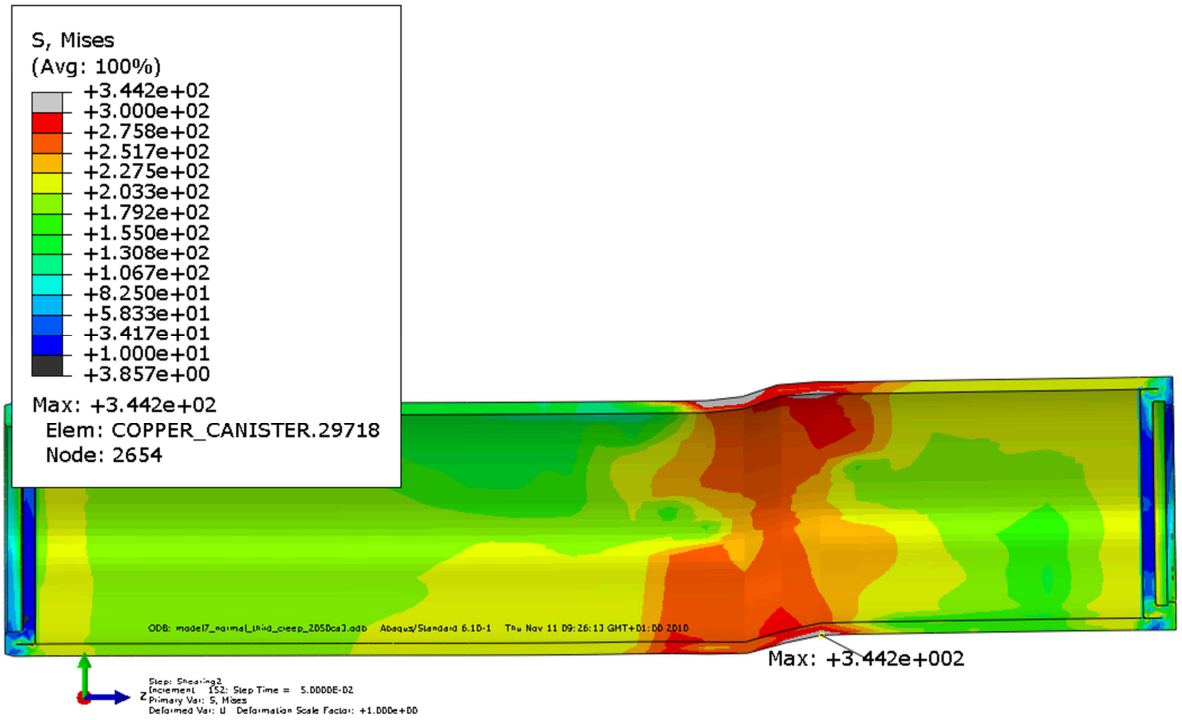

Figure A3-4. *Mises stress for copper shell - 10 cm shearing magnitude.*

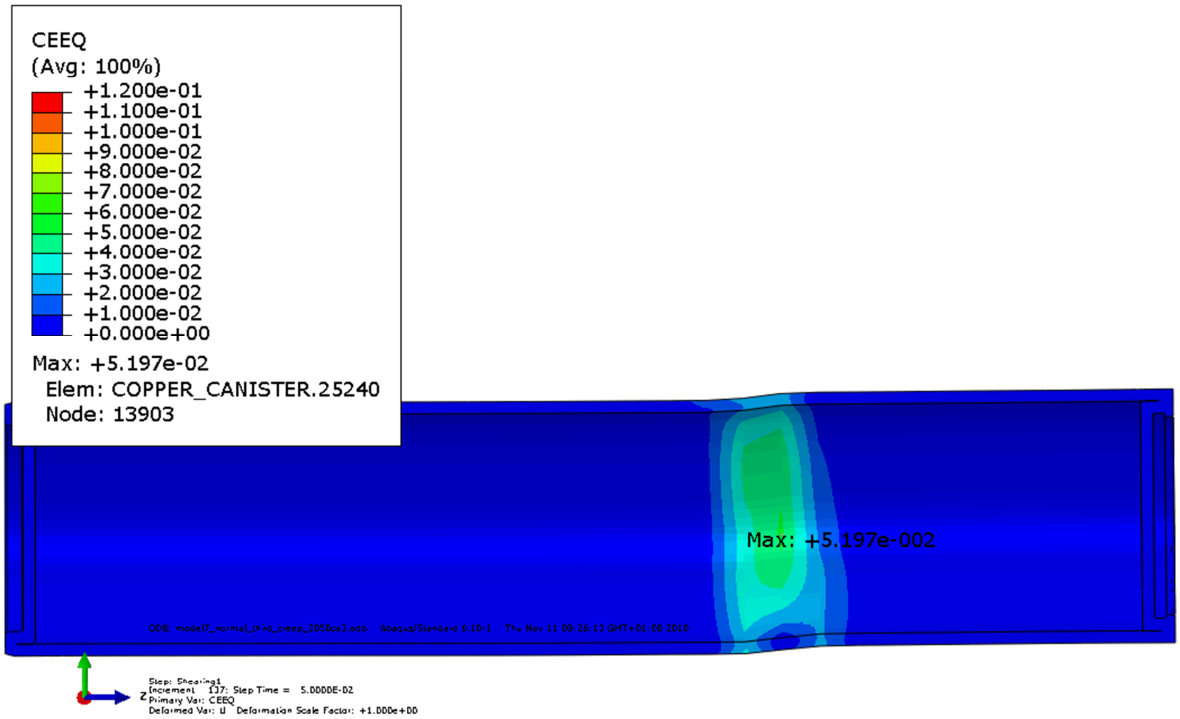

Figure A3-5. *Creep strain (CEEQ) for copper shell - 5 cm shearing magnitude.*

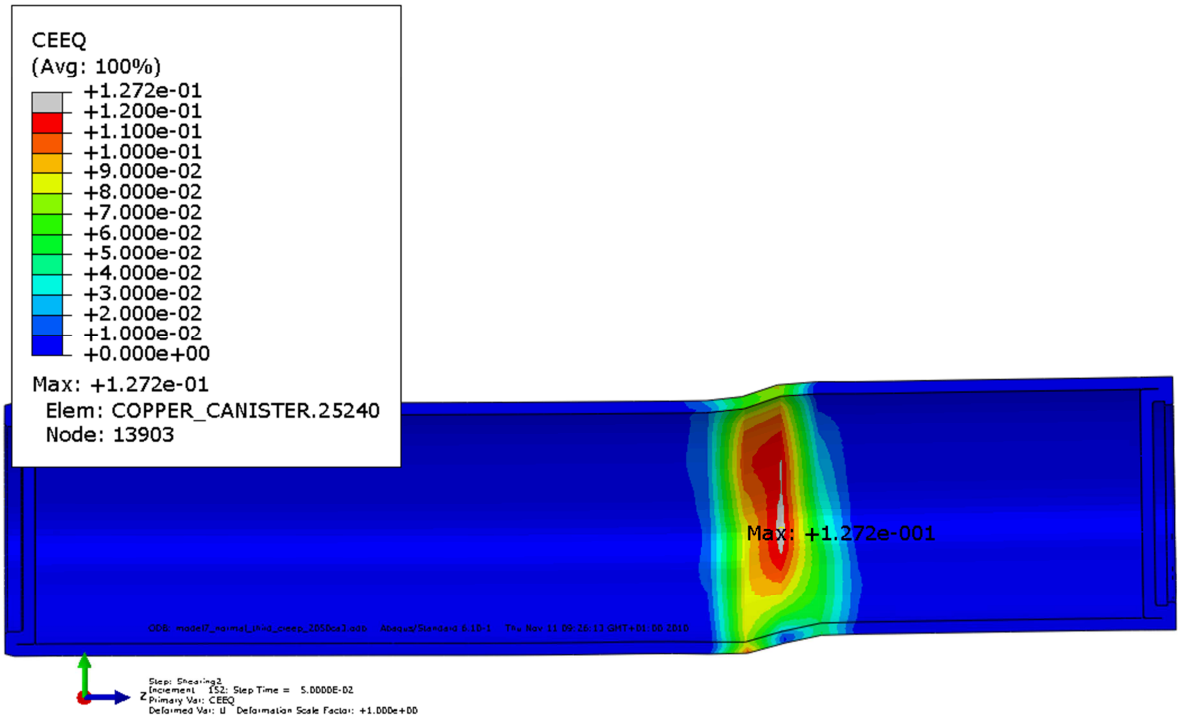

Figure A3-6. *Creep strain (CEEQ) for copper shell - 10 cm shearing magnitude.*

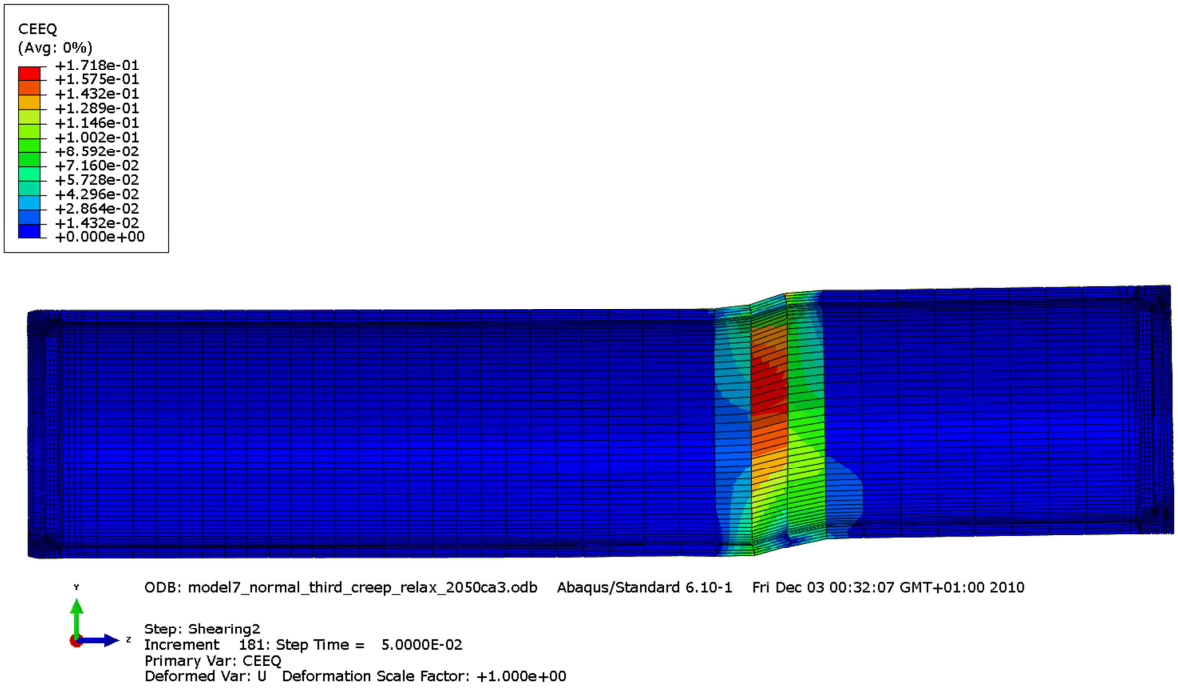

Figure A3-7. *Creep strain (CEEQ) in copper shell after10 cm shearing (no averaging, compare with Figure A3-6).*

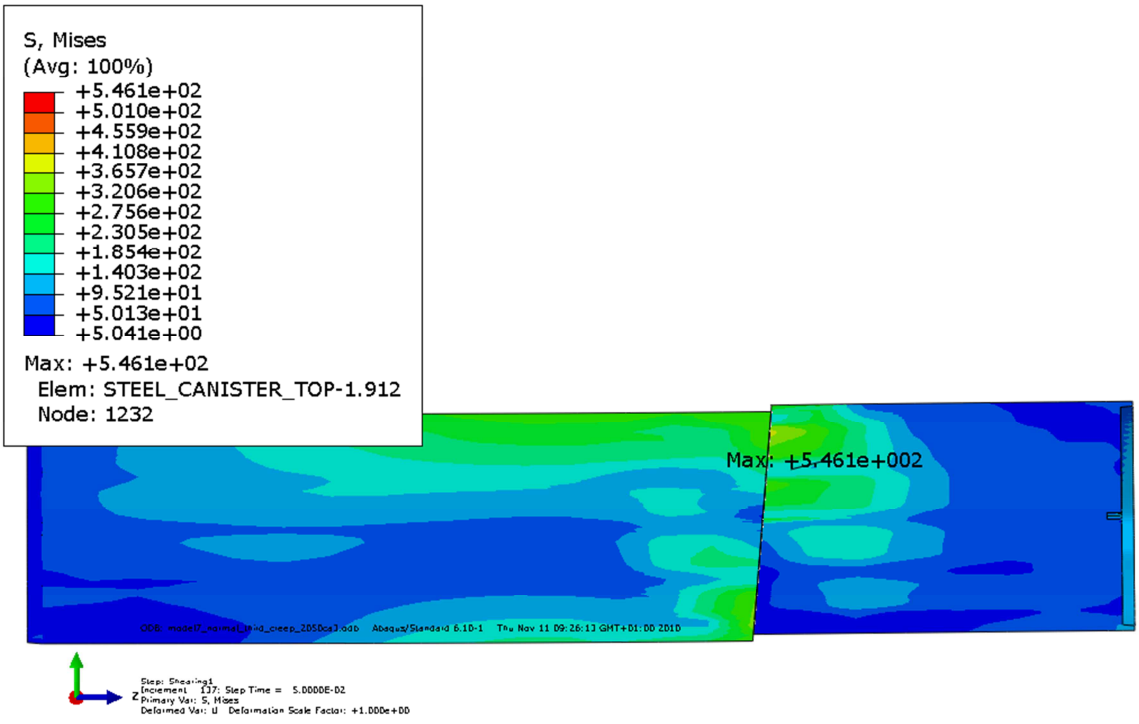

Figure A3-8. *Mises stress for insert - 5 cm shearing magnitude.*

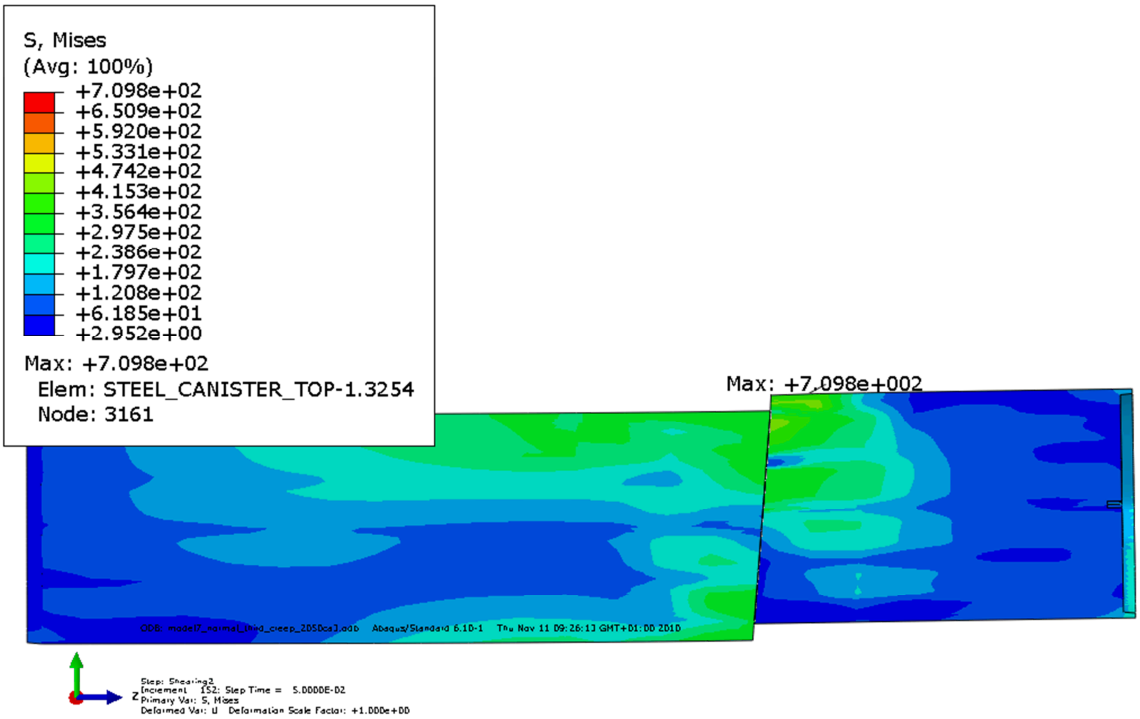

Figure A3-9. *Mises stress for insert - 10 cm shearing magnitude.*

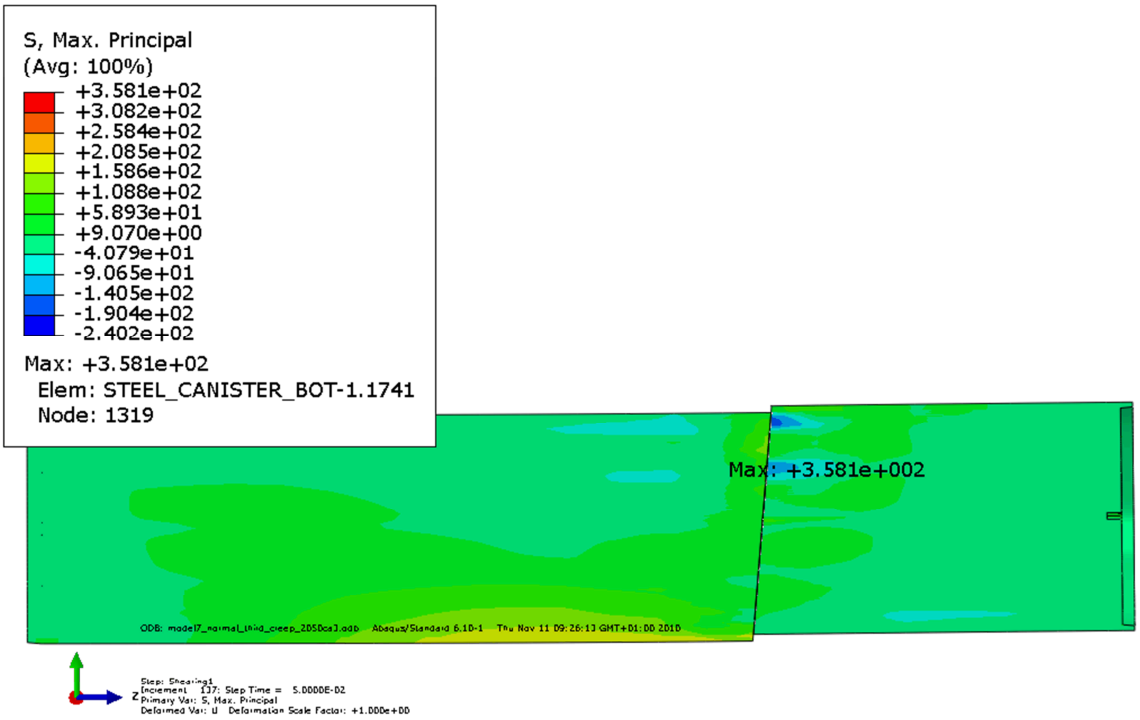

Figure A3-10. *Max principal stress for insert - 5 cm shearing magnitude.*

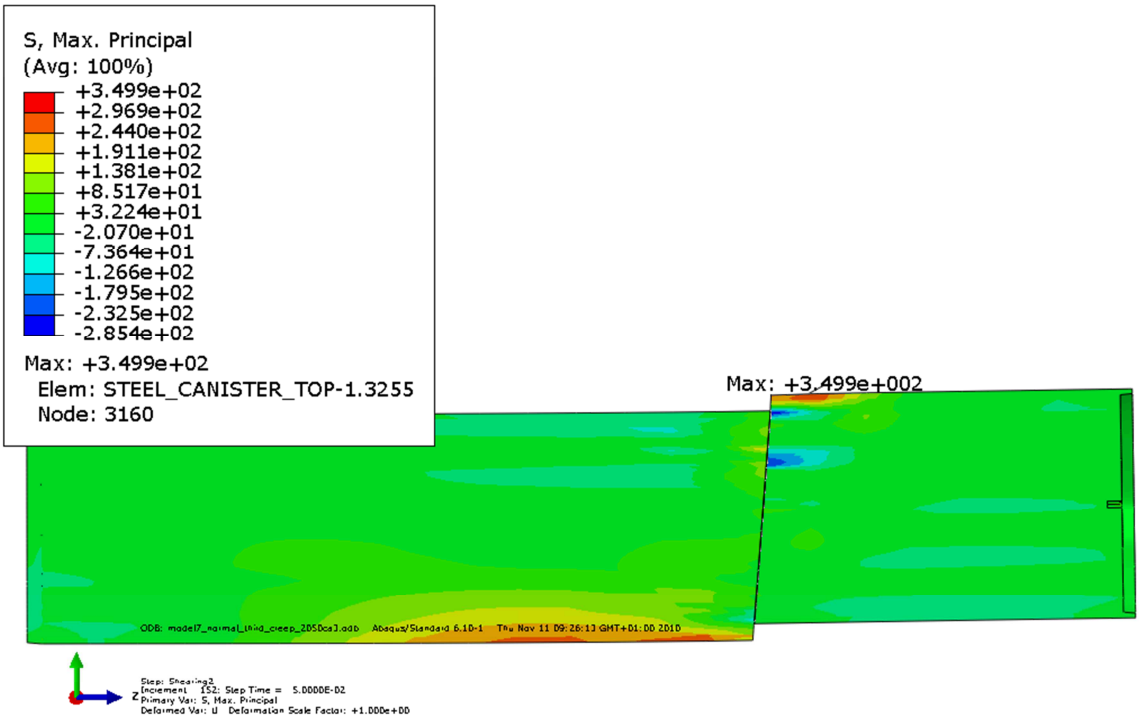

Figure A3-11. *Max principal stress for insert - 10 cm shearing magnitude.*

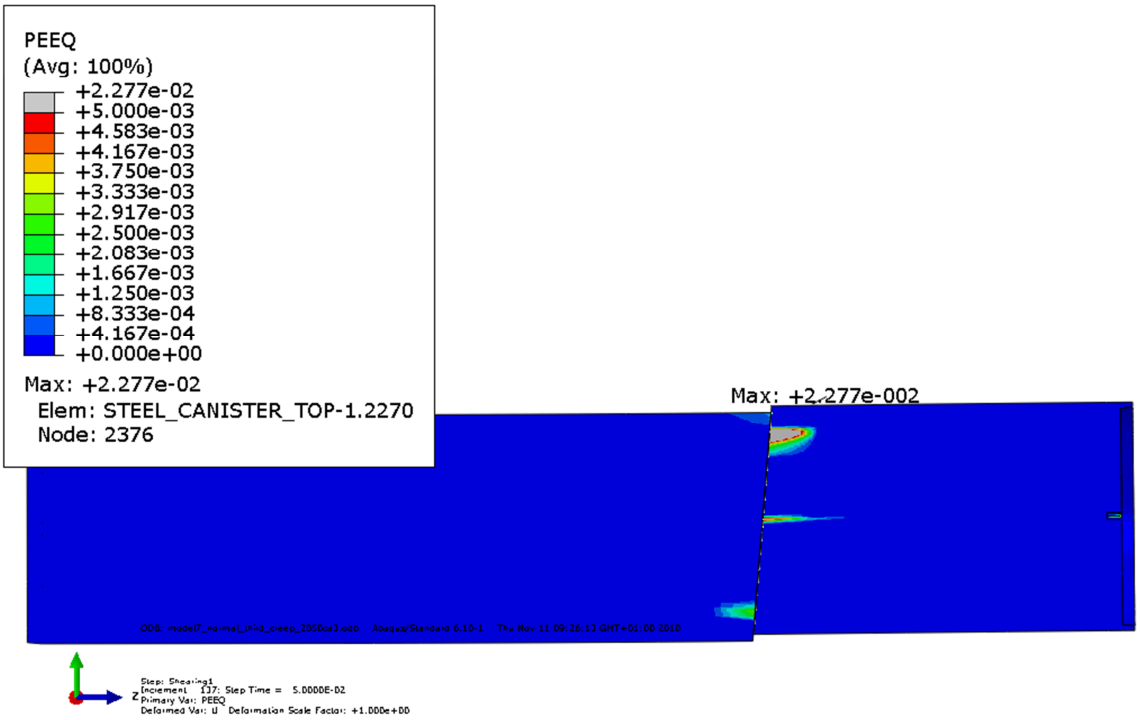

Figure A3-12*. Plastic strain (PEEQ) for insert - 5 cm shearing magnitude.*

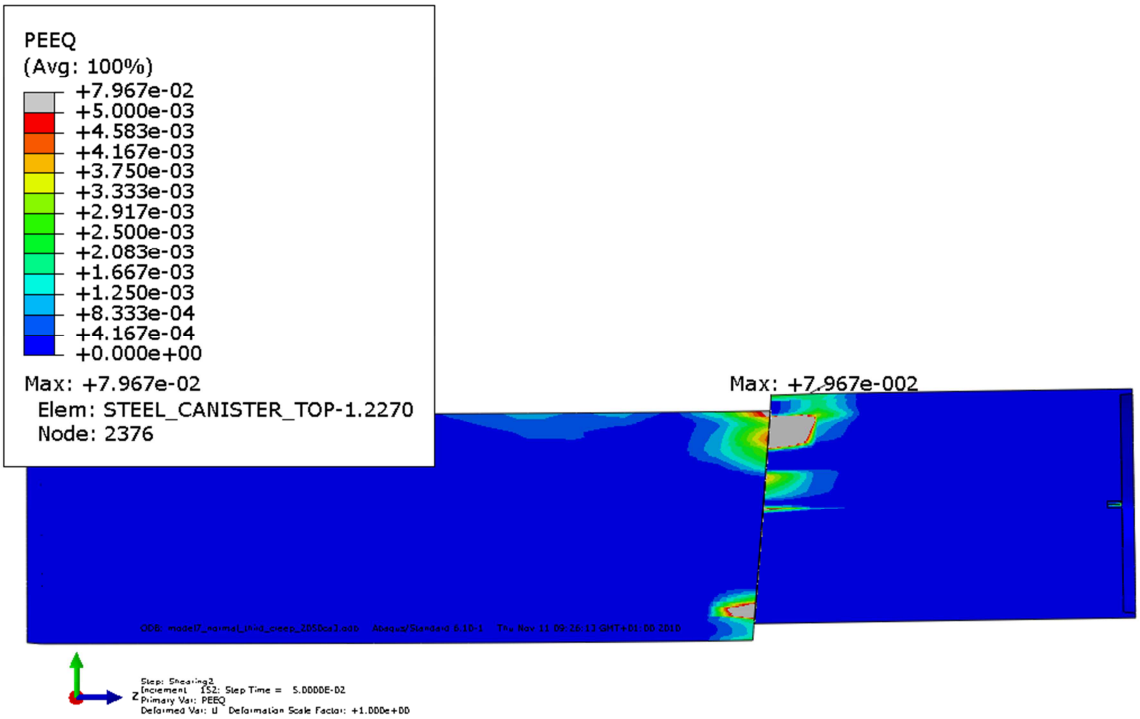

Figure A3-13. *Plastic strain (PEEQ) for insert - 10 cm shearing magnitude.*

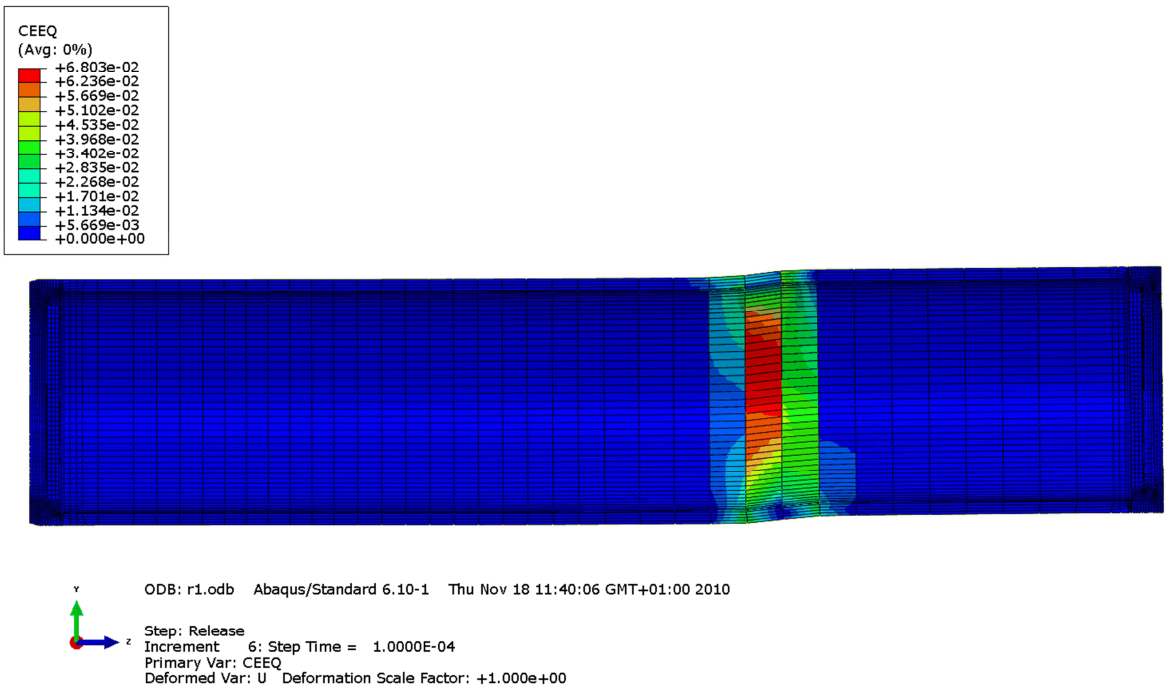

Figure A3-14. *Creep strain (CEEQ) in copper shell after 5cm shearing – buffer removed.*

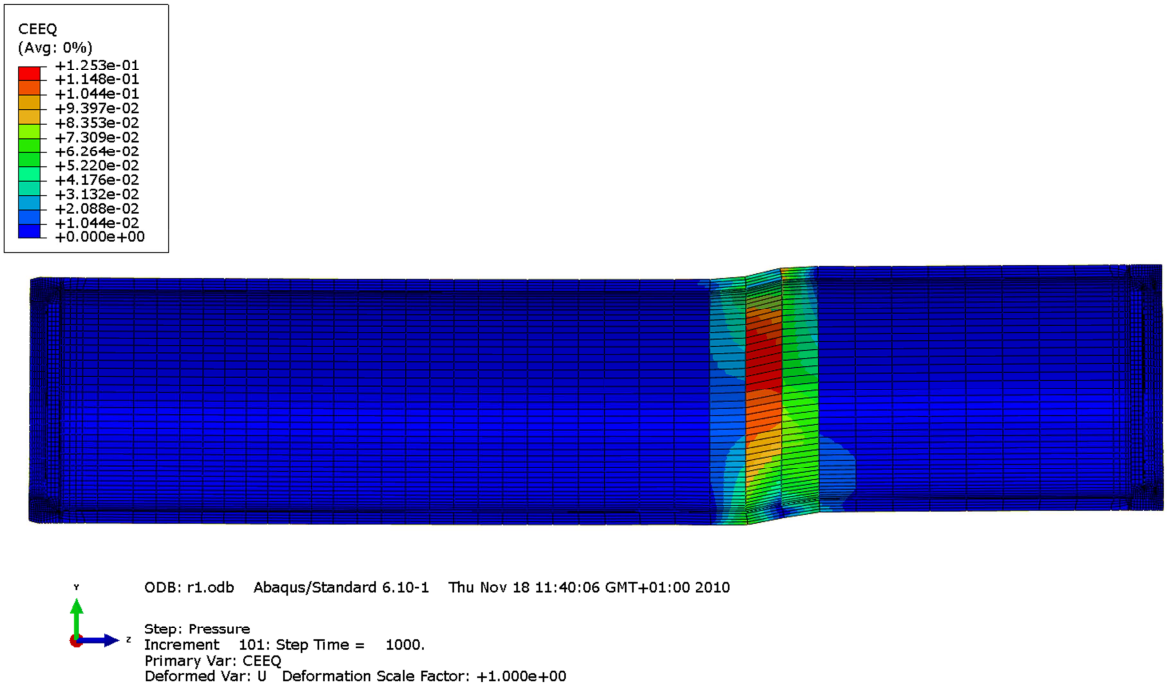

Figure A3-15. *Creep strain (CEEQ) in copper shell after 10 cm shearing – buffer removed.*

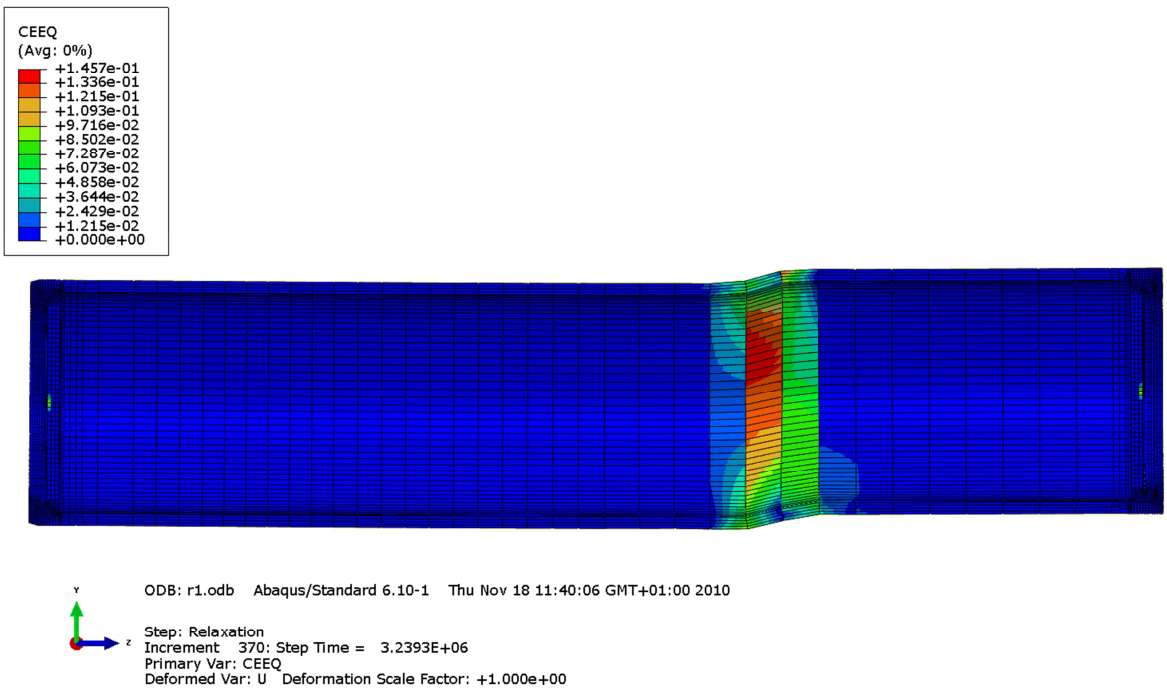

Figure A3-16. *Long term creep strain (CEEQ) in copper shell after 10 cm shearing (36 days) – buffer removed.*

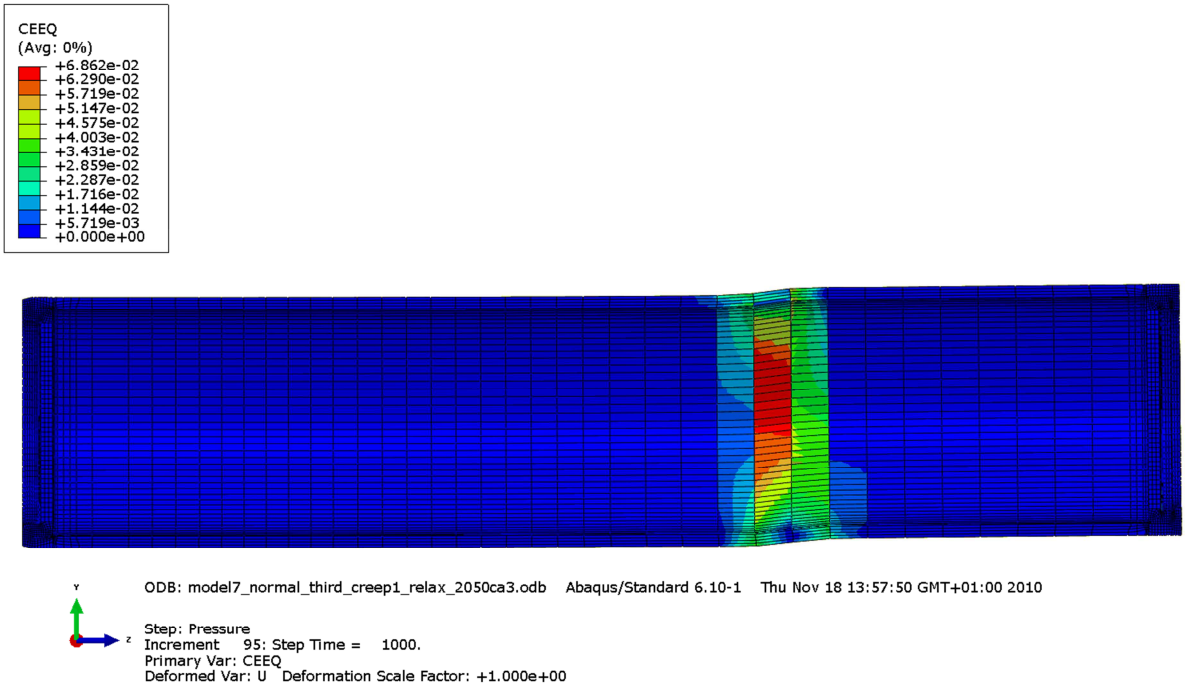

Figure A3-17. *Creep strain (CEEQ) in copper shell after 5 cm shearing and applied pressure (15MPa).*

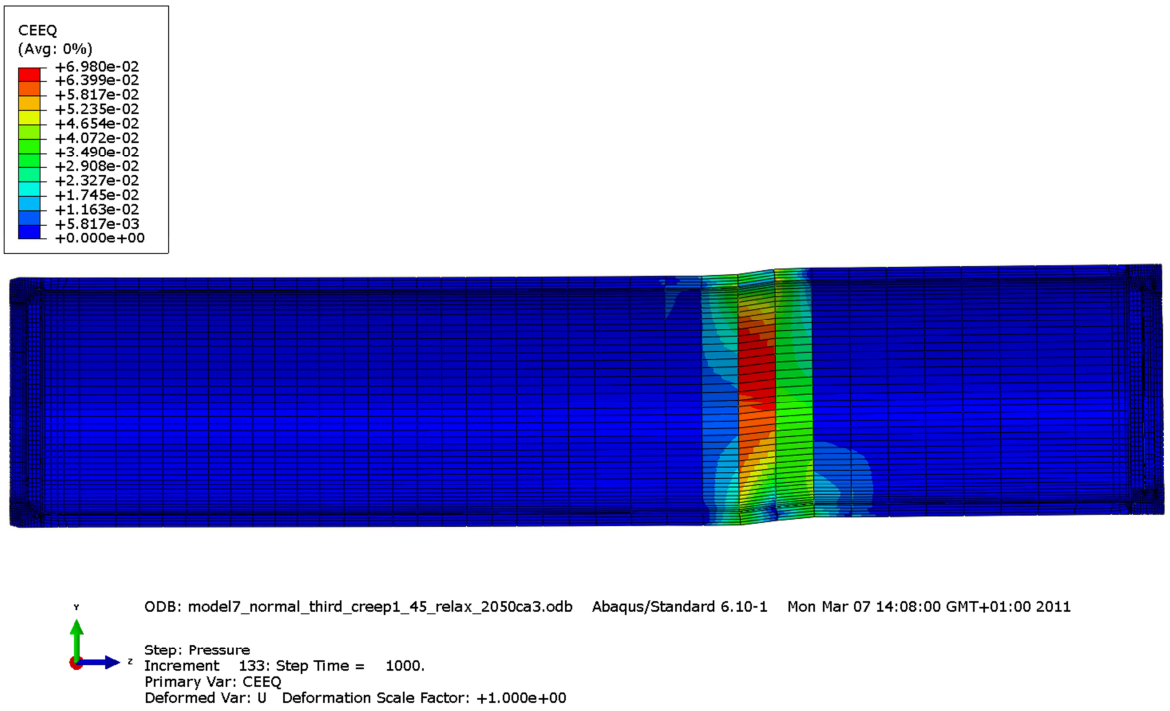

Figure A3-18*. Creep strain (CEEQ) in copper shell after 5 cm shearing and applied pressure (45MPa).*

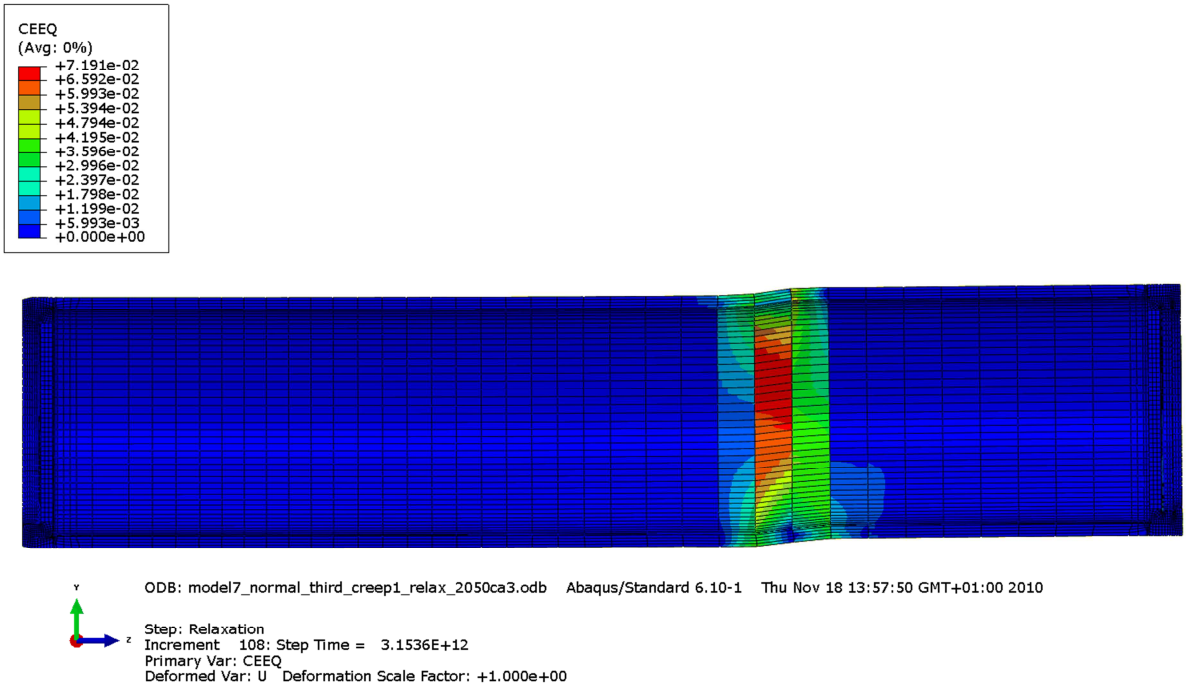

Figure A3-19. *Long term (100,000 years) creep strain (CEEQ) in copper shell after 5 cm shearing and applied pressure (15 MPa).*

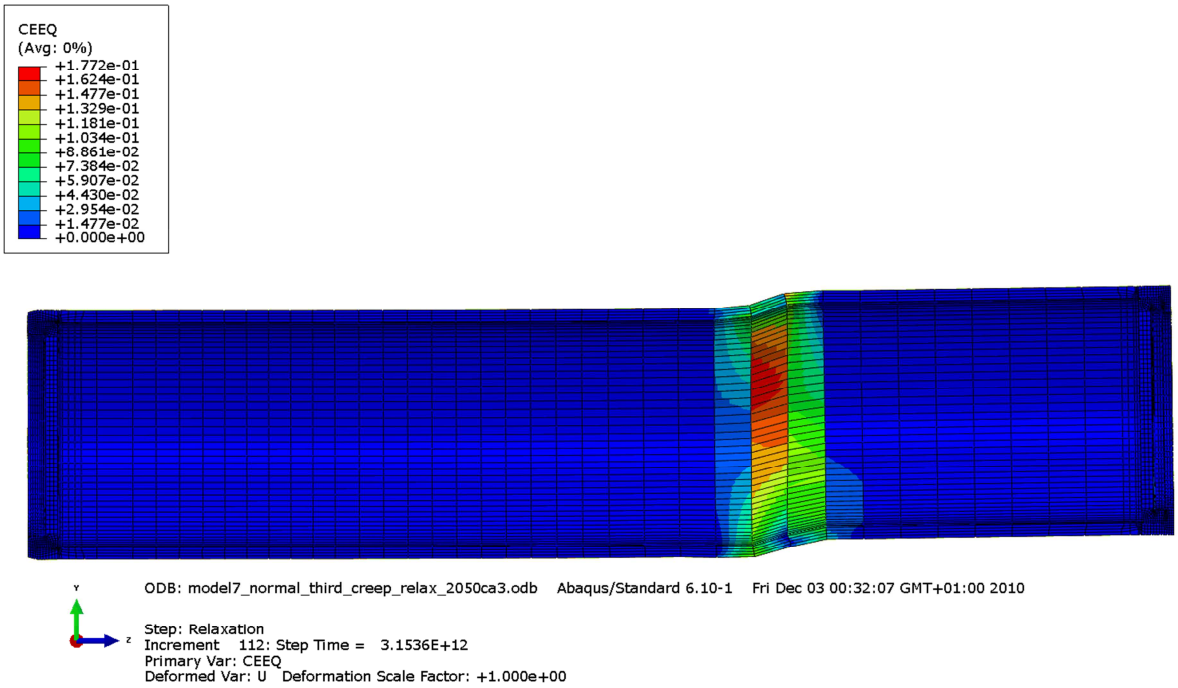

Figure A3-20. *Long term (100,000 years) creep strain (CEEQ) in copper shell after 10 cm shearing and applied pressure (15 MPa).*

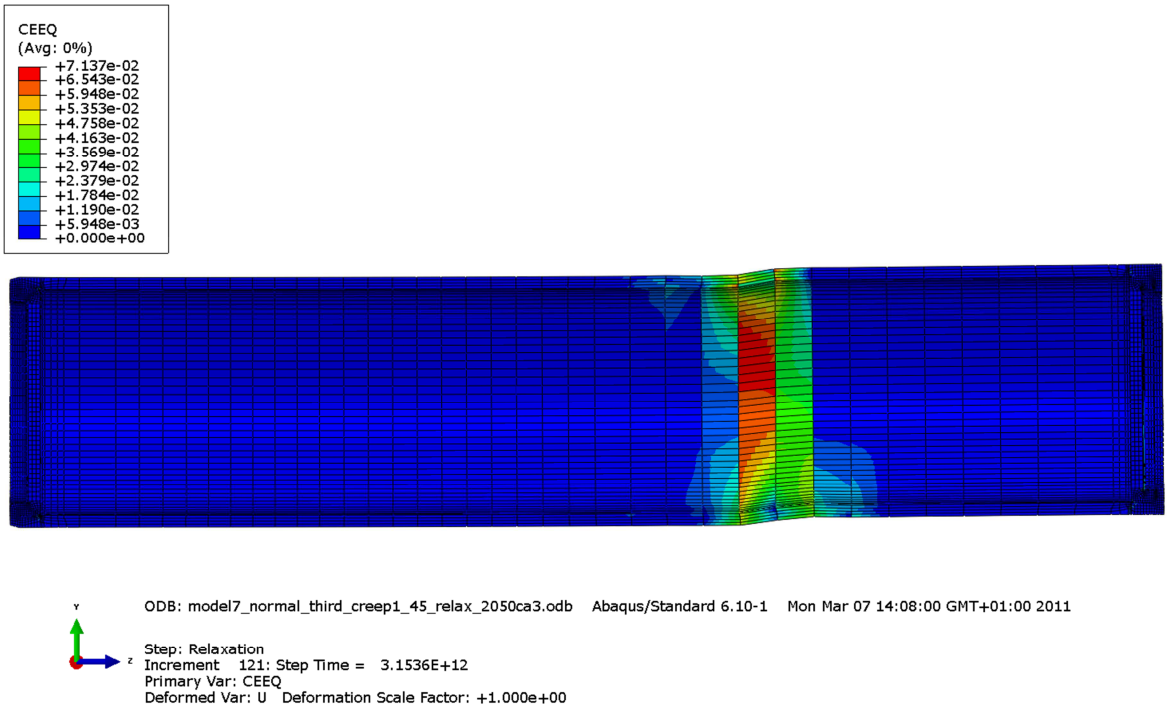

Figure A3-21. *Long term (100,000 years) creep strain (CEEQ) in copper shell after 5 cm shearing and applied pressure (45 MPa).*

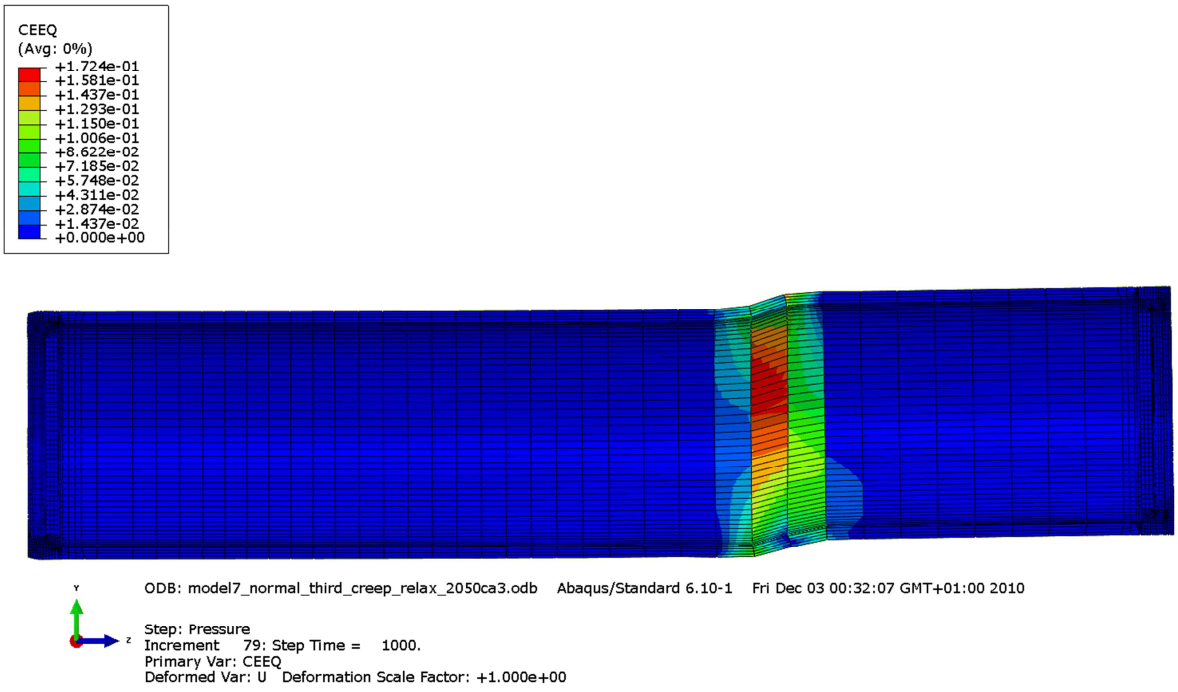

Figure A3-22. *Creep strain (CEEQ) in copper shell after 10 cm shearing and applied pressure (15 MPa).*

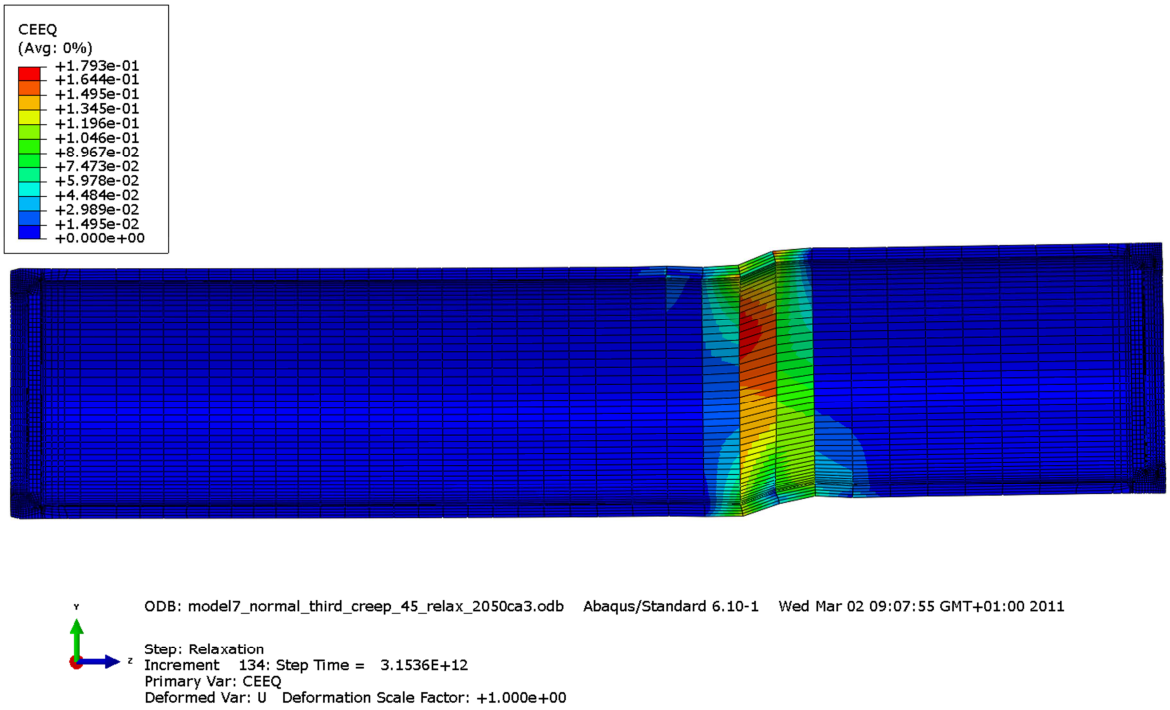

Figure A3-23. *Long term (100,000 years) creep strain (CEEQ) in copper shell after10 cm shearing and applied pressure (45 MPa).*

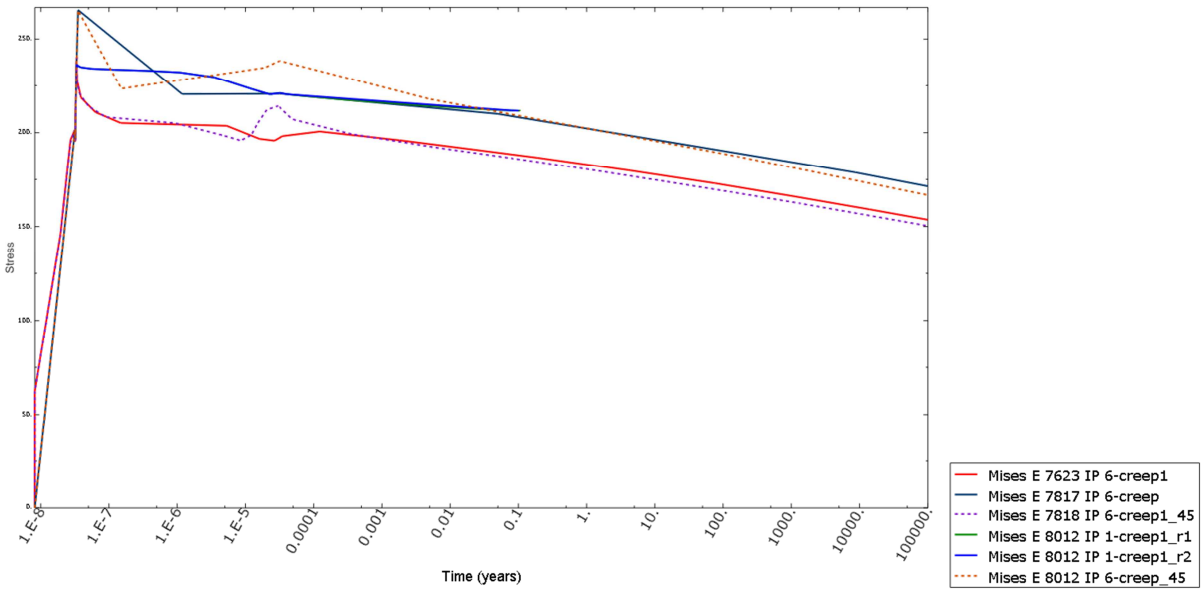

Figure A3-24. *Mises relaxation for one selected point having maximum creep strain (CEEQ) (with and without buffer). Curves ending at time 0.1 years represents the approach with buffer removed. With buffer active the pressure load 15 MPa (solid lines) or 45 MPa (dashed lines) imply almost identical results. 5 cm (red,cyan) or 10 cm (blue,yellow,green) shearing gives significant difference.*

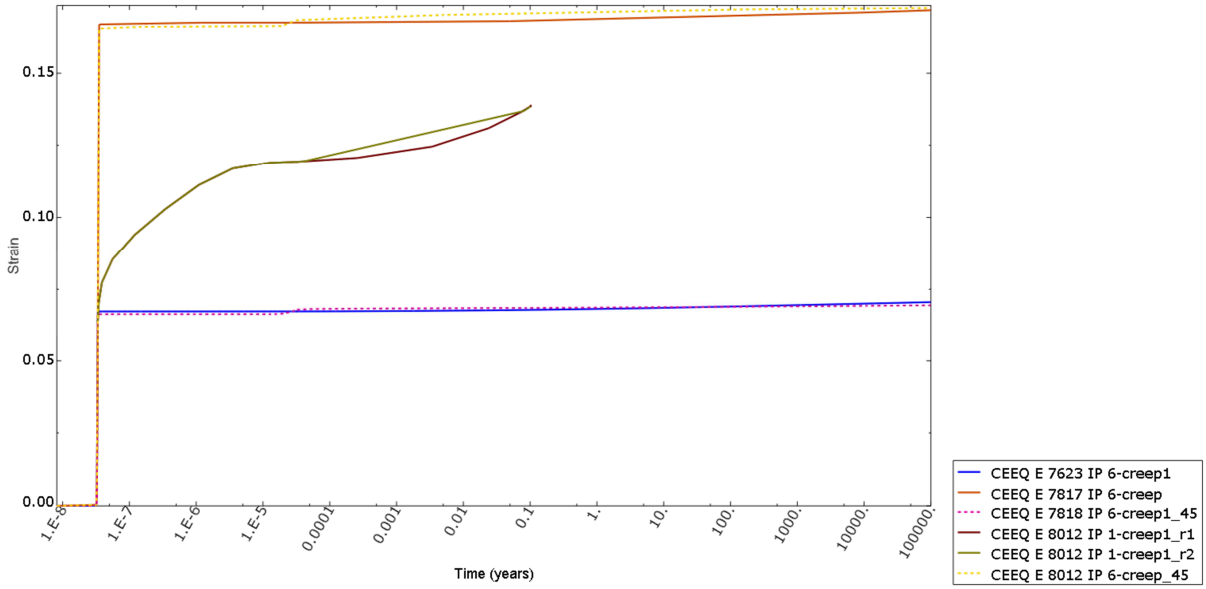

Figure A3-25. *Creep strain (CEEQ) for one selected point having maximum creep strain (with and without buffer). Curves ending at time 0.1 years (36 days) represents the approach with buffer removed. With buffer active the pressure load 15 MPa (solid lines) or 45 MPa (dashed lines) imply almost identical results. 5 cm (blue,cyan) or 10 cm (green,red,yellow,orange) shearing gives significant difference.*